UCRL-84632
PREPRINT

CONF-801104--4

SOME CHEMICAL ENGINEERING CHALLENGES IN DRIVING THERMOCHEMICAL HYDROGEN PROCESSES WITH THE TANDEM MIRROR REACTOR

Terry R. Galloway
Richard W. Werner

MASTER

THIS PAPER WAS PREPARED FOR SUBMITTAL TO THE
73rd Meeting
of the
American Institute of Chemical Engineers
November 16-20, 1980
Chicago, Ill.

November 10, 1980

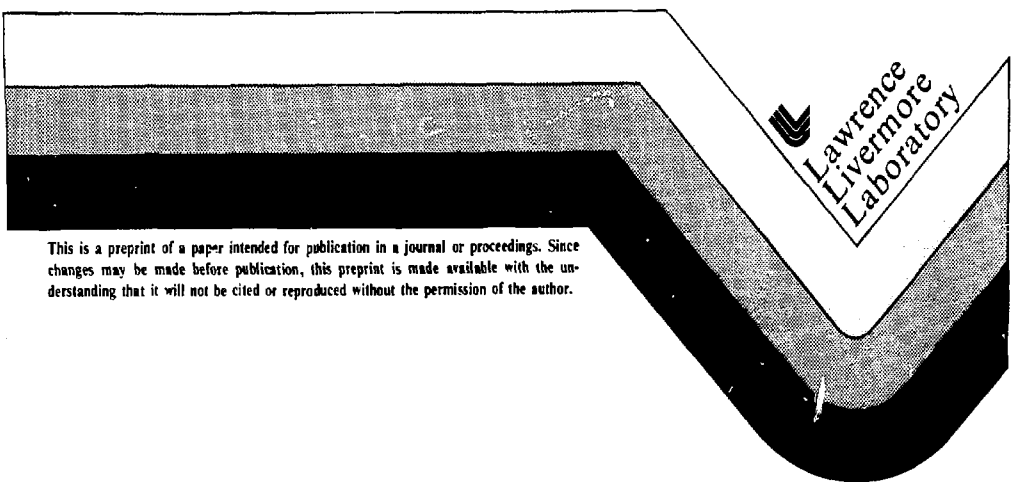

SOME CHEMICAL ENGINEERING CHALLENGES IN DRIVING THERMOCHEMICAL HYDROGEN PROCESSES WITH THE TANDEM MIRROR REACTOR*

Terry R. Galloway and Richard W. Werner
Lawrence Livermore National Laboratory
Livermore, California 94550

ABSTRACT

We present the highlights of our design study whose objective is to determine how the magnetic fusion program, and the future Tandem Mirror Reactor (TMR), can benefit and support the production of synthetic, portable fuels that are vital to the economy of the U.S. In the case under study the reactor is used as a 1200K heat source driving a thermochemical cycle whose output product is hydrogen. Principal focus for the reactor energy source is placed on the conceptual design of the blanket module. The module under study is a Li-Na Cauldron design which consists of a binary, liquid metal pool boiler that uses lithium as the neutron moderator and sodium vapor as the heat transfer fluid with the latent heat of vaporization of sodium providing the main mode of energy transport.

The Tandem Mirror Reactor is described and compared with Tokamaks, both from a basic physics viewpoint and from the suitability of the respective reactor for synfuel production. Differences and similarities between the TMR as an electricity producer or a synfuel producer are also cited.

The thermochemical cycle chosen to link with the fusion energy source is the General Atomic Sulfur-Iodine Cycle, which is a purely thermal-driven process with no electrochemical steps. There are real chemical engineering challenges of getting this high quality heat into the large thermochemical plant in an efficient manner. We illustrate with some of our approaches to providing process heat via liquid sodium to drive a 1050 K, highly-endothermic, catalytic and fluidized-bed SO_3 Decomposition Reactor. The technical, economic, and safety tradeoffs that arise are discussed.

*Work performed under the auspices of the U. S. Department of Energy by the Lawrence Livermore Laboratory under contract number W-7405-ENG-48

INTRODUCTION

Introduction - Why NOW For Fusion and Synfuels

The study of fusion energy had its origins with the Atomic Energy Commission roughly some 30 years ago. That was a time when a reactor and electrical energy production made an obviously good combination. Oil was fifty cents a barrel, the OPEC did not exist, our post-war industrial complex was expanding and requiring more electrical energy, and the few compact cars that existed were driven by eccentrics rather than economists.

Today, the picture has changed. The demand for electricity has leveled off with a growth rate lower than our economic growth. Our average national electric generating capacity is more than adequate. There may remain local shortages of electrical generating capacity but becoming more dominant is the need for fuel to drive them. Compact cars are commonplace.

Fuel prices have skyrocketed, with crude oil at $30/barrel and rising. Inflation and an unstable economy, due largely to an increasing world demand for a decreasing oil resource is almost universal. Responsible people in the U.S. saw this energy problem coming at least 15 years ago. Due to inertia, and other problems we failed to act until just recently. The nation has finally started, albeit a bit late, on a national energy plan and a substantial synthetic fuel program. Those of us in the fusion community must not suffer from the same inertia and must become part of this energy plan and part of the synfuel venture now, not later, even though our reactor may be 20 or 25 years down the pike. It is time to actively include synthetic fuel production in the fusion program. We have made some progress in this area.

Technical Justification

Based on U.S. energy needs we believe that fusion should and must play as strong a role in the production of fuels and chemical feedstocks as it is expected to play in the production of electricity. The role, in fact, may be even stronger since the production of fuel in the form of hydrogen, hydrocarbons, and their derivatives useful for transportation, industrial processes, or for residential and commerical use or the production of chemicals based on hydrogen or hydrocarbons is three times as high in the U.S. as is the use of energy for the production of electricity. This energy distribution is illustrated in Fig. 1 for the year 2000.

We further believe that fuel production is not inimical to electricity production from fusion but is complementary to it and strengthens the base of the entire fusion program.

Notice in Fig. 1 the areas in which Fusion/Synfuels can have a large impact on the U. S. energy demands. Synthetic pipeline gas derived from H_2 can be used for residential, commercial or industrial needs. Hydrogen, methanol, or other hydrocarbons can be used as transportation fuels.

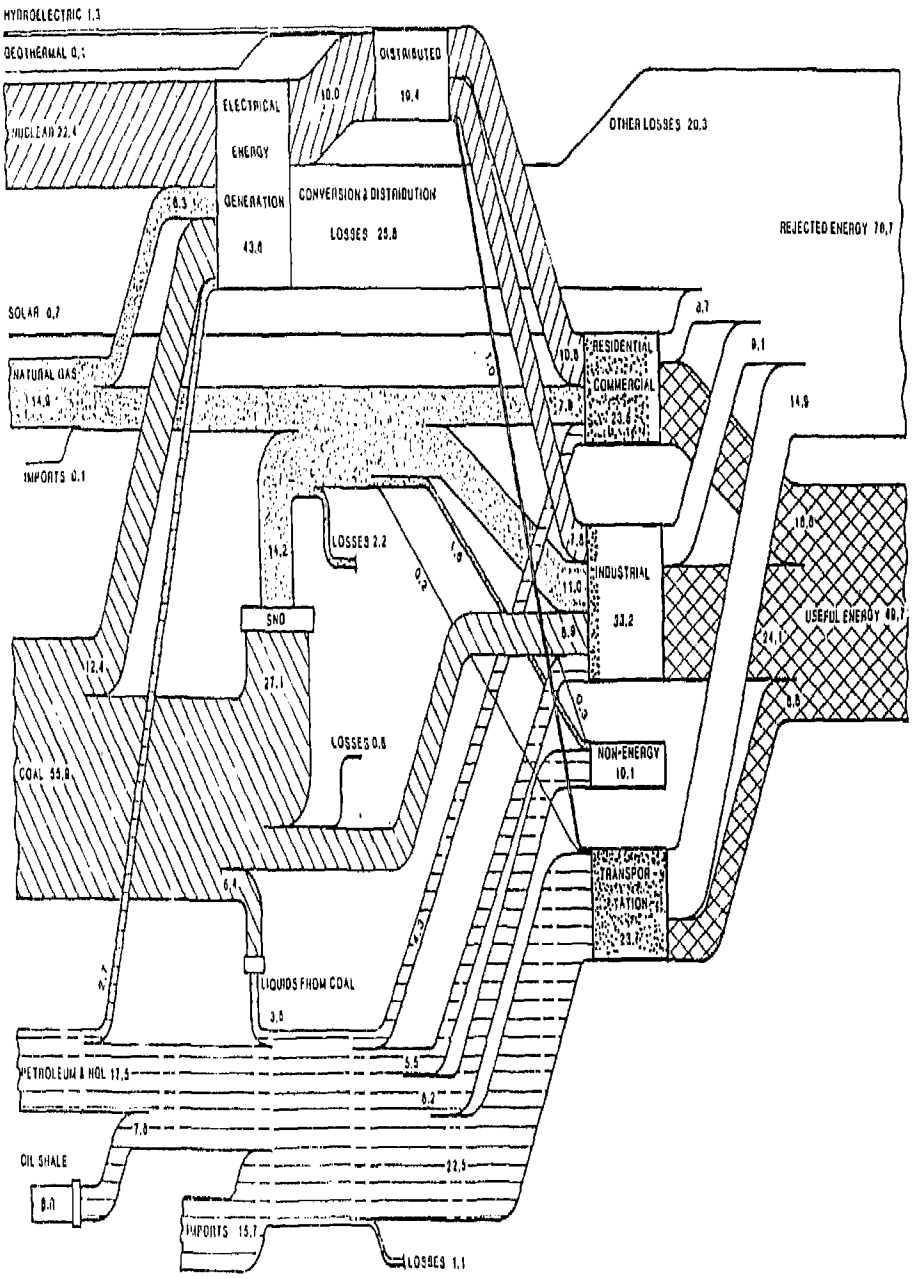

Fig. 1. U.S. energy-flow diagram for year 2000 (end-use and supply R,D&D case, primary-resource consumption 136.6 quad). With intensive R,D&D primary-resource consumption is reduced by 13% due to improved end-use efficiencies and conservation practices. Synthetic liquids and gases from coal and shale are more significant and imports are greatly reduced. The stipled area indicates the potential impact that can be made by fusion-syn fuels.

In Fig. 2 we show our estimate of world wide energy flows, which was synthesized from a large variety of published sources[1-7] together with our own longterm estimates. Note that as our carbon-based (fossil) sources are depleted a large demand for fusion-synfuels appears around 2030, some 15 years after fusion-generated electricity is introduced around 2015. Around 2030 (coal supplies are large and will still be available, although slightly declining in volume and increasing in price). Synthetic fuels whether carbon-based liquids or straight gases (cryogenic- or hydrid-stored) require fusion-generated hydrogen. Hydrogen is the first key step that must be provided for the world energy demands to be met in a transitional economy going from fossil fuels to the inexhaustibles. Fusion heat can also be used for coal or oil shale production by replacing the process heat needs that would otherwise need to come from combustion of those valuable resources.

Our Tandem Mirror Fusion Reactor driving a thermochemical hydrogen plant could fill this need via the RD&D program laid out in Fig. 3.

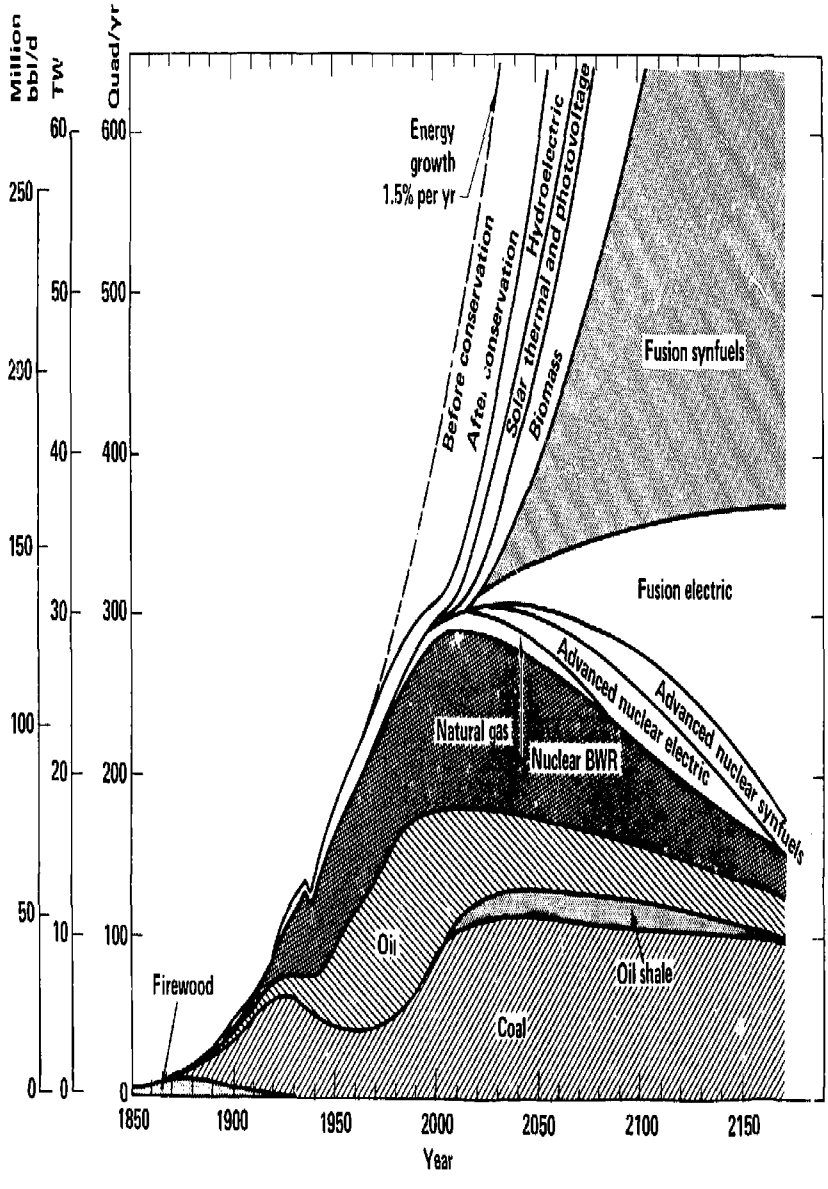

Fig. 2. Worldwide energy flows.

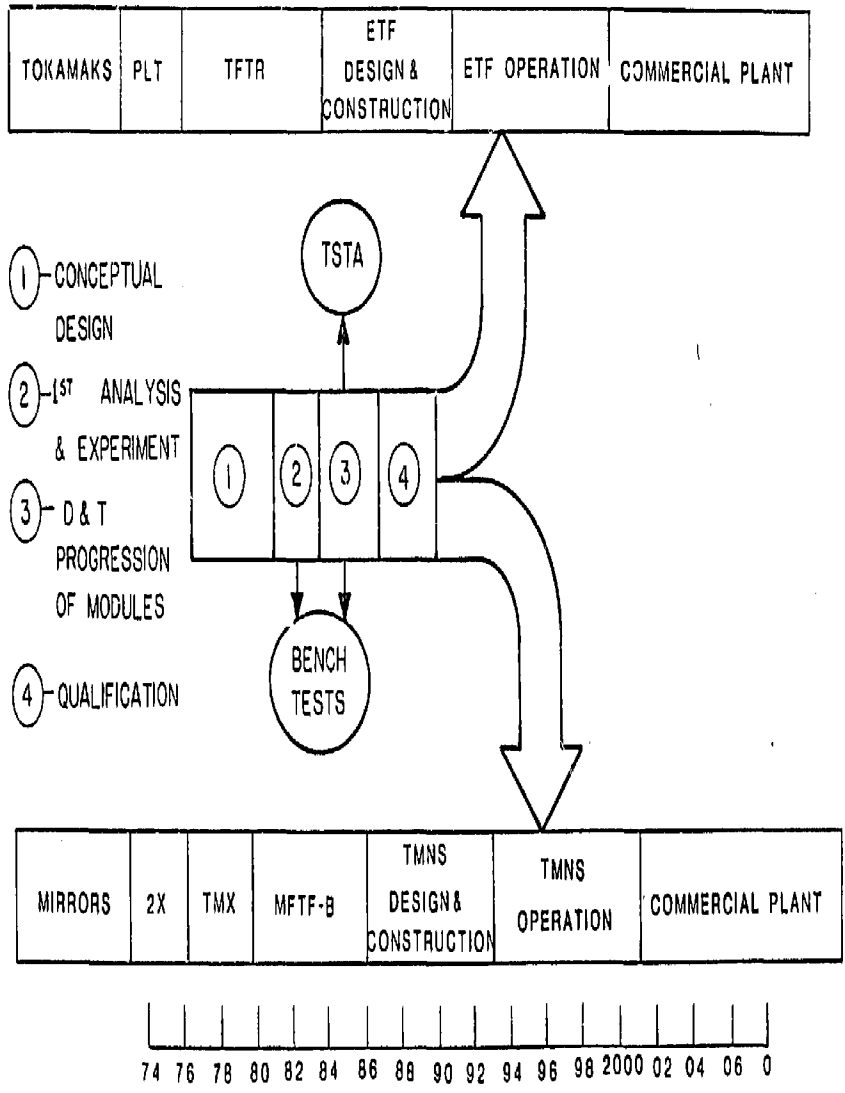

Fig. 3. Fusion/thermochemical link plan.

PRODUCTION OF SYNTHETIC FUELS AND CHEMICALS

HYDROGEN AS THE FIRST CRITICAL STEP

In the early 1970s the development of hydrogen technology reached such a level that its use for a chemical raw material, heating, lighting, transportation and chemical energy seemed plausible. As a result the concept of the "hydrogen economy" developed. A schematic representation of the "hydrogen economy" is shown in Fig. 4. [2] Although many of these concepts have not been technically or economically established, the potential is worthy of consideration.

A primary energy source such as nuclear fission, fusion, or solar is used to produce H_2 as the portable energy carrier. H_2 would be distributed by pipeline, stored in underground vessels as a gas or in smaller vessels as a cryogenic liquid. H_2 as a heating fuel offers the advantage that it can be efficiently burned catalytically ("flameless") at temperatures as low as the end use, without the need for inefficient flues, or the formation of NO_x. An "all-hydrogen" home could use "condoluminescence" lighting where H_2 excites a cold phosphor to a bright luminescence. H_2 can more efficiently meet the variable (peak power vs time) energy load of society by means of transport, storage, and fuel cell regeneration of electricity as needed, in contrast to the problems our fossil-based power plants have operating away from full-rated load. Also as a transition plan cogeneration plants producing electric power and electrolytic H_2 have particular advantages. As a transportation fuel H_2 is excellent but offers storage problems, thus, methanol may be a better alternate.

The production of H_2 can be by electrolytic or thermochemical splitting of water. Present-day electrolytic plants operate at around 60 to 70% efficiency using electricity generated from heat at efficiencies around 35 to 40%. Thus, overall H_2 thermal efficiencies around 21 to 28% are realized. New high-pressure high-temperature electrolytic cell designs for aqueous electrolysis promise cell efficiencies around 85%--thus, raising the overall H_2 thermal efficiency to about 29-34%.

The incentive for thermochemically produced H_2 is that presently demonstrated bench-scale units promise around 50% efficiency for the process. Thus, thermochemical cycles are viable competition to the high-pressure high-temperature electrolytic cell now under development.

NON-RENEWABLE CARBON-BASED FUELS

The largest use of H_2 today is as a chemical raw material in the chemical, petrochemical, and petroleum industries. Coal and oil shale industries, now in rapid growth, are expected to use H_2 at massive levels. Nearly all of this H_2 demand, however, is met by steam-reforming or partial oxidation of fossil raw material feed. For these applications H_2 is not produced remotely and transported to the plant. Obviously large increases in

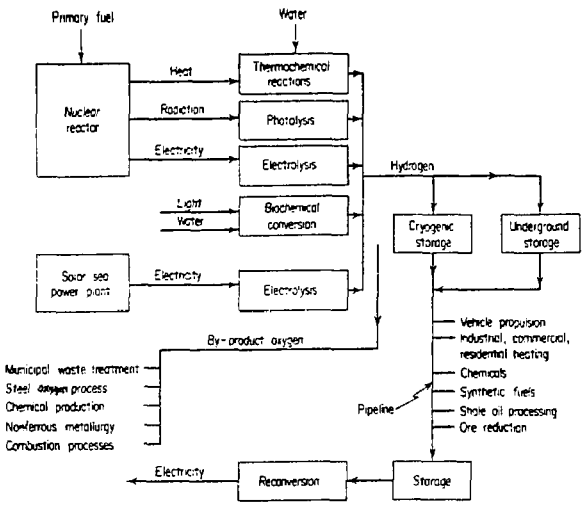

Fig. 4. A schematic view of the "hydrogen economy" (Ref. 2).

the value of fossil, non-renewable carbon-based raw materials would be needed to justify the use of electrolytically or thermochemically generated H_2. Undoubtedly the time will come where carbon sources will be too valuable to burn and H_2 will be required for these industries.

RENEWABLE CARBON-BASED FUELS

Beyond ~2030 carbon sources may become so valuable and rare that H_2 may be needed to drive a carbonate- or CO_2-based industry producing methanol or other hydrocarbons required for our economy's carbon-based chemical needs. CO_2-sources in minerals, CO_2 wells, stack gases, oceans or the atmosphere are technically feasible. A plant using renewable CO_2 and H_2 might manufacture, for example, methanol for a transportation fuel and a raw chemical feed. Combustion of methanol to $CO_2 + H_2O$ would then be released to the biosphere to complete a closed cycle where CO_2 build-up may no longer be an environmental concern.

TMR PHYSICS AND BLANKET ENGINEERING

The Technical Choice of the TMR

The fusion reactor as an energy source was critical to our study, and we investigated how well fusion might produce synthetic fuels, as well as what influence the fuel production would have on basic reactor design.

It can be stated that the main influence synfuel production had on reactor design had to do with blanket modules, those units surrounding the plasma that convert the neutrons' kinetic energy to thermal energy and in the case of the D-T cycle also produce the tritium part of the fuel by neutron-lithium reactions. Blanket modules satisfactory for synfuel production use must run hot, ~1200K; whereas blanket modules for electrical production could run hot but need not, ~750K is representative, thus thermochemical cycles influence on the reactor is non-trivial and introduces difficult problems in high temperature design not only of the module but its associated heat exchangers and transport piping. Materials problems arise as a consequence. Other engineering elements of the reactor remain substantially the same as they would be for electrical production. The physics may be slightly easier due to the basic size of a fusion reactor for synfuels compared to one for electical production. The synfuel plant is larger by perhaps a factor of two and thus the reactor Q, the figure of merit defined as Fusion Power Output/Injected Power, can become higher. Economics of scale are also implied by the larger size.

TMR Design Parameters - Thermochemical Hydrogen vs. Electrical Production

Table 1 provides a comparison between a conceptual reactor design for fuel production and one for electrical production.

Assembly, Disassembly and Accessibility

A primary technical reason for choosing the tandem mirror was its highly favorable reactor configuration. The configuration not only allows the design of structurally simple blanket modules that are the principal source of the process heat but puts them together into a workable package.

Figures 5, 6, 7 and 8 illustrate how the blanket modules, tailored for synfuel thermochemical cycle use may be assembled into a highly manageable, serviceable, accessible reactor for producing energy.

The Reactor Blanket Designs

Two basic blanket module concepts were considered in this study. One is the Li-Na Cauldron blanket. The other is the flowing microsphere design.

TABLE 1

Example Design Parameters for the Tandem Mirror Reactor

For Synfuel Production or Electrical Production

		Synfuel	Elec.
Fusion Power	(MW_f)	5680	3500
Thermal Power	(MW_t)	4945	3360
First Wall Loading	(MW_t/m^2)	2.0	2.6
ECRH Power Delivered	(MW)	330	260
Neutral Beam Power Delivered			
Central Cell	(MW)	0.0	0
Barrier Cell	(MW)	85	58
Plug	(MW)	8.5	48
Central Cell Length	(m)	260	125
Central Cell Fist Wall Radius	(m)	1.4	1.7
Global Reactor Q-Value		13.3	9.6
P_{net}	(MW_e)	0	1000
β_c		0.4	0.4
Bc	(T)	~2	~2
B_p	(t)	~12	~12

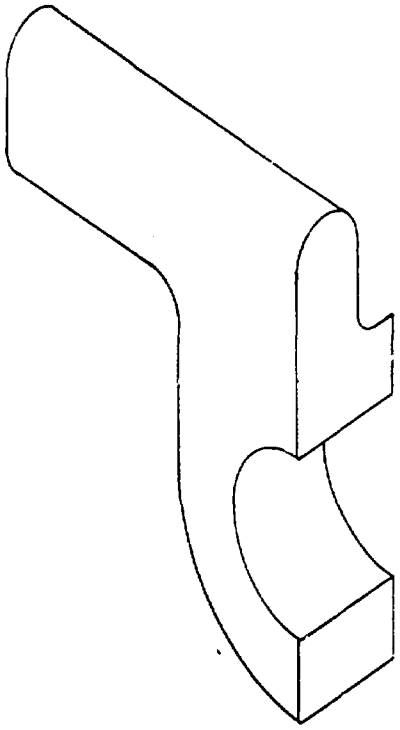

Fig. 5A. Basic geometry of a Cauldron blanket module.

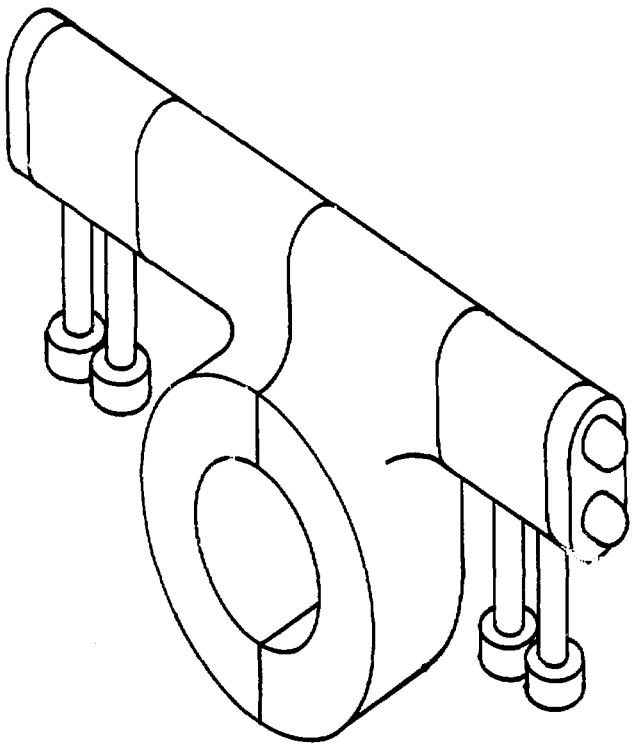

Fig. 5B. The two modules joined and ready for assembly with a central cell solenoid.

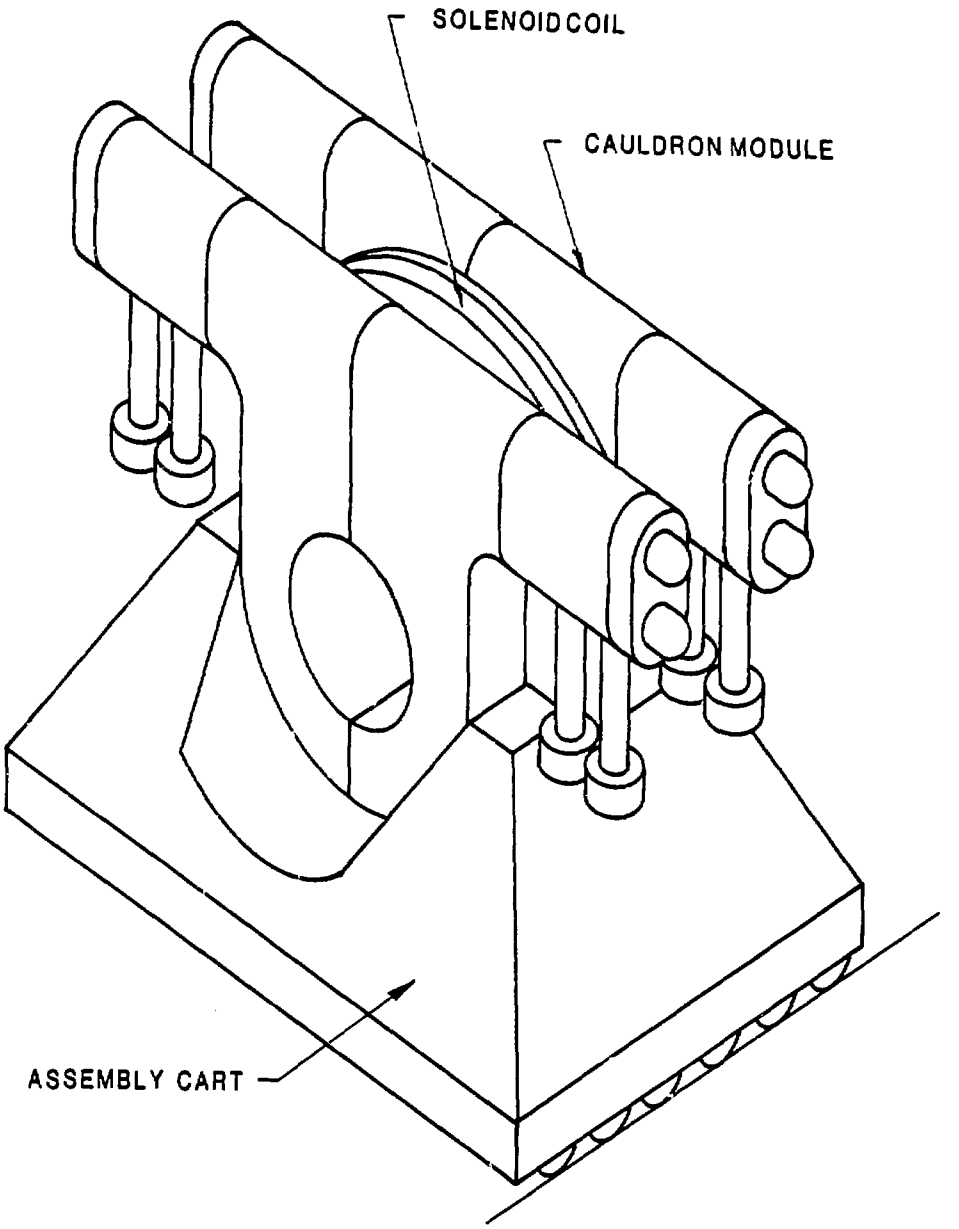

Fig. 6. Four modules and a solenoid coil assembled into a unit cell.

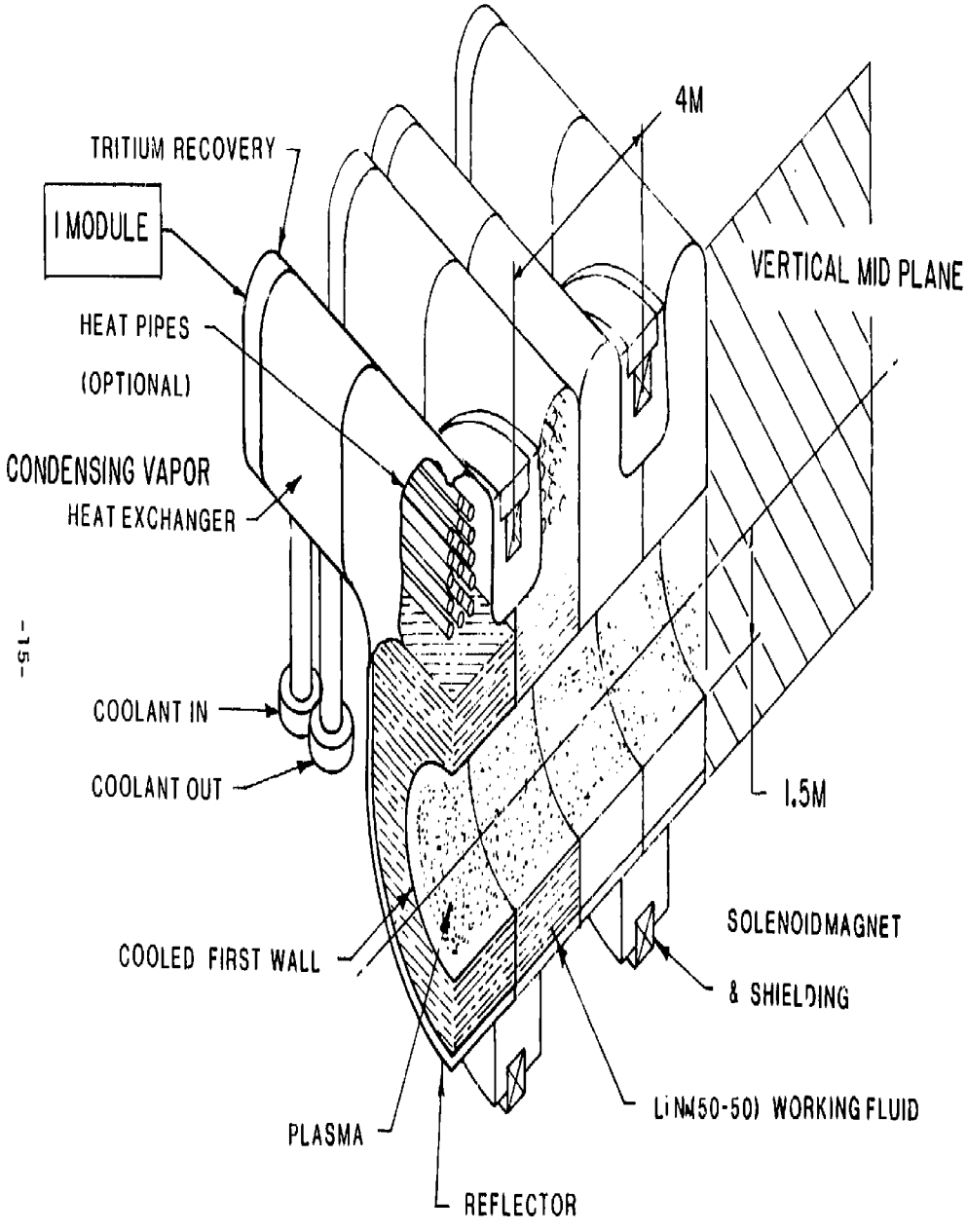

Fig. 7. Cross section through two unit cells of the TMR. Each unit cell consists of four blanket modules and one solenoidal coil. The unit cells are joined in series to form the main central cell of the reactor.

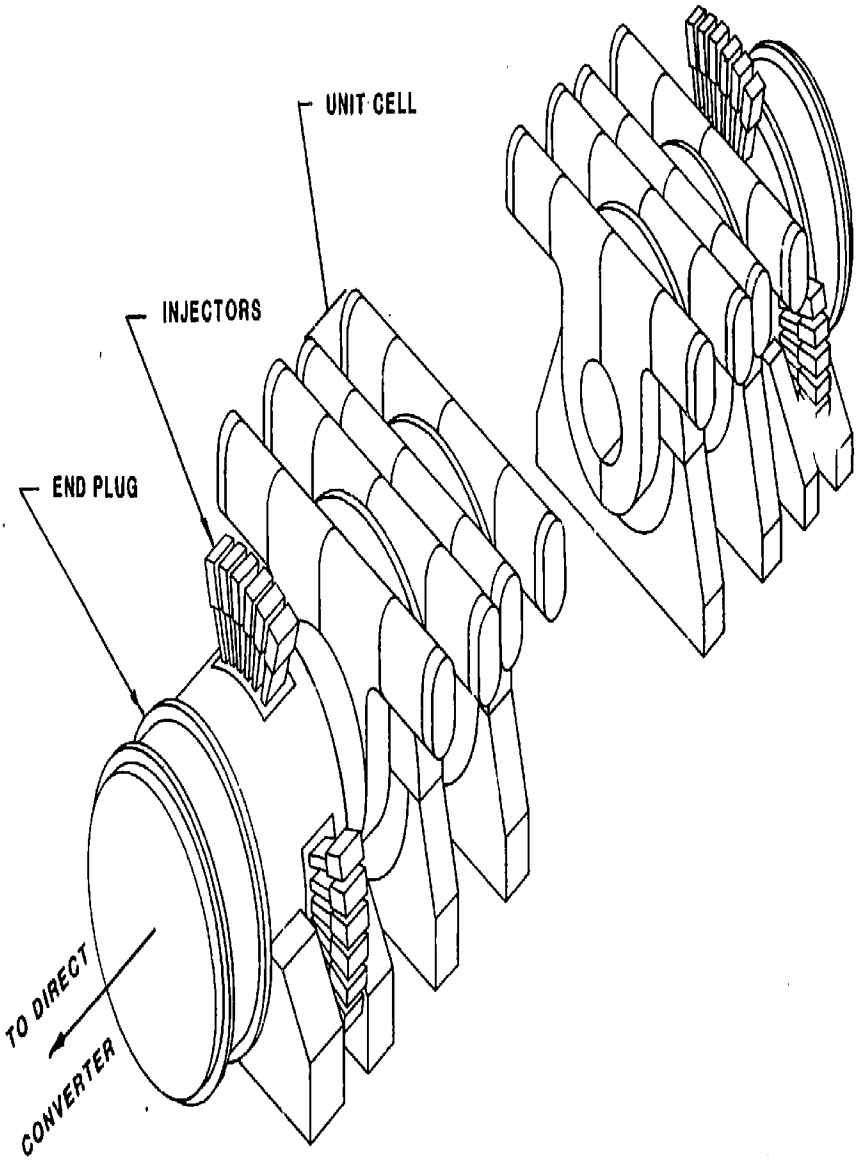

Fig. 8. A highly simplified illustration of how the TMR would be assembled with end plugs, injectors, unit cells, etc. The direct convertor is not shown.

The Operating Principle of the Cauldron Blanket Module

A cross-sectional view of the Cauldron module is illustrated in Fig. 9. Notice the module's resemblance to a pool boiler. It is, however, substantially more complicated than a pool boiler due to geometric effects, due to the exponential energy generation in the fluid contained within the module and, last but not least, due to MHD effects on the convective mixing of the two liquid metals, lithium and sodium, we have chosen to use in the pool. The two liquids in this Cauldron module act as both the neutron moderator and heat transfer fluid, absorbing energy in direct proportion to the energy input and transferring it by latent heat of vaporization of the sodium to a heat exchanger in the dome of the vessel. The lithium performs the function of tritium breeding. In the dome the condensing vapor heat exchanger (CVHX) transfers the thermal energy out of the module to various chemical processors located some distance from the reactor.

The sodium preferentially vaporizes, leaving behind the lithium in the liquid state to do its neutron moderating, tritium-producing function. The sodium vapor, traveling at vapor velocities roughly 8-10 m/s at 1200 K, condenses on the heat exchanger tubes in the dome, yields energy and returns as liquid droplets to the pool, thus completing the cycle. We have selected the Li-Na mixture for our studies, and an alternate possibility is Li-K. The two fluids, lithium and sodium, are miscible and the tritium breeding ratio with a 50-50 mix is greater than 1. The neutronics of the potassium is a little less favorable although the Li-K can run cooler for the same vapor velocity. Li-Rb or Li-Cs are other mixtures or compounds that may be of future interest.

The Tandem Mirror Reactor Physics Base

The tandem (TMR) is a steady state, driven fusion device. It operates for the purposes of this study on the deuterium-tritium cycle. Energy from the reactor is produced in two primary forms as evidenced by equation (1).

$$D + T \rightarrow n\ (14.1\ \text{Mev}) + {}^4\text{He}\ (3.5\ \text{Mev.}) \qquad (1)$$

Deuterium + Tritium → Energetic Neutron + Charged Particle

The first energy form, the kinetic energy of the neutron, is captured in the moderating blanket surrounding the reacting plasma and thermal energy is produced. The cylindrical plasma is physically located in the TMR's central cell in a zone that is about 200 meters long for this synfuel production application. The plasma is contained within the central cell by the retarding action of the mirror end cells whose electrostatic potential causes the deuterium and tritium ions to be reflected back and forth sufficiently long so that some of them react with one another and fuse.

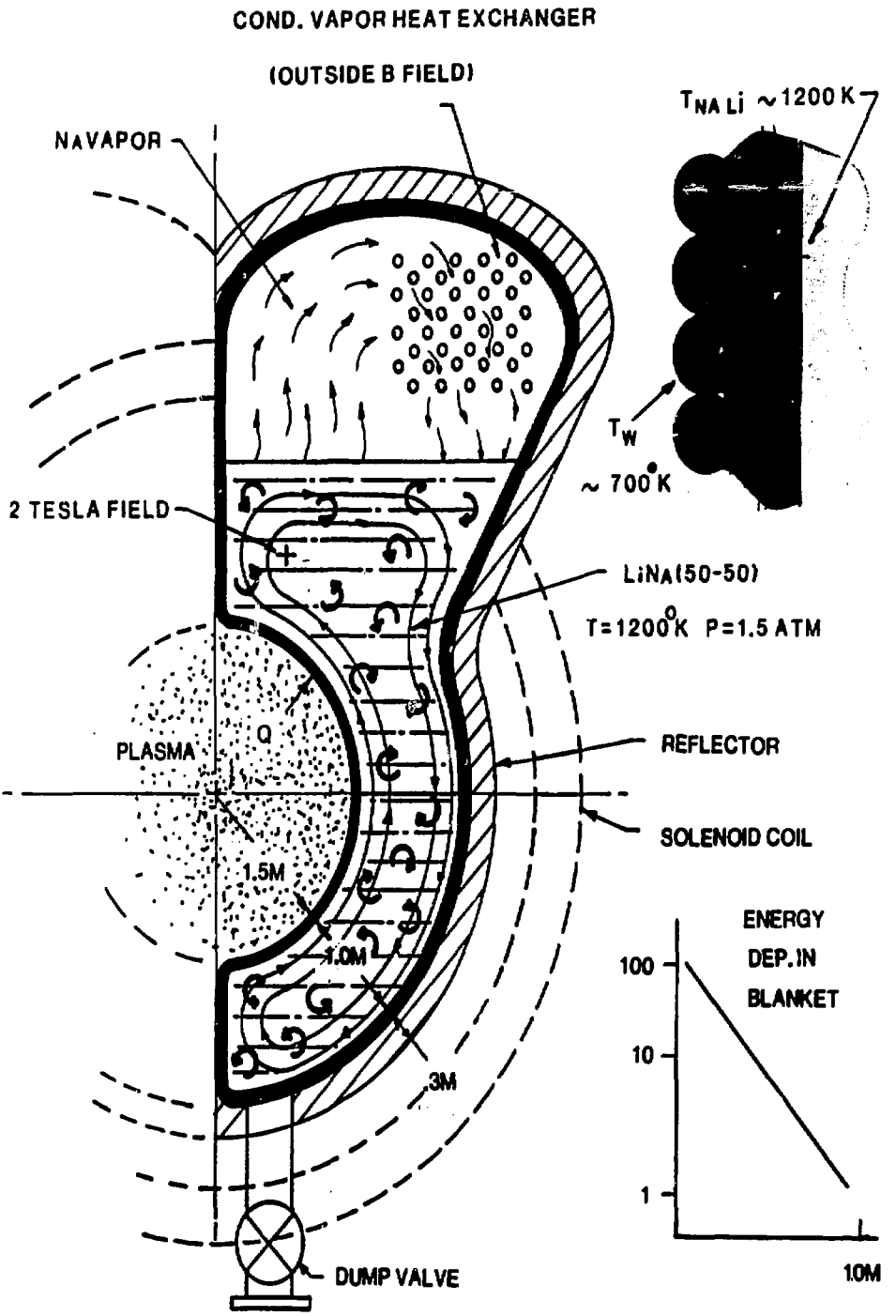

Fig. 9. The Cauldron concept-housing a hot fluid in a cool container.

The second energy form produced by the reactor is that contained in the charged alpha particle. On forming, the alpha begins to lose some of its 3.5 Mev energy by heating the plasma through a series of collisions with electrons and ions. Finally, at some degraded energy, the alpha particle leaves the system (the central cell) through the ends as do the deuterium and tritium ions that did not react with one another. All the alpha particle energy may now be accounted for as the sum of its residual energy plus the enhanced energy of the exiting deuterium and tritium ions. This energy is recovered in a direct convertor located beyond the end cells. The direct convertor produces two forms of energy, an electrical dc component which we use in our point design to drive the reactor, and a thermal component which, for our thermochemical cycle, furnishes energy for process chemistry. The neutrons, as they are moderated in the blanket, produce some additional energy by exothermic neutron-lithium reactions.

The Uniqueness of the TMR

There is a uniqueness associated with the Tandem Mirror Reactor open-ended physics geometry that increases the usefulness of this energy source over other contemporary energy producers such as solar energy concentrators, Tokamaks, and high temperature gas cooled fission reactors (HTGR) for the production of synthetic fuels. This uniqueness has to do with the fact that in the TMR, open-ended mirror geometry there is a direct convertor which produces dc power that may be used in thermochemical cycles to meet the electrical demand and/or the needs of an electrolysis step. The result of using the direct convertor is an improvement in overall efficiency as schematically illustrated in Figs. 10A and 10B.

The Influence of Q on the TMR's Uniqueness

To illustrate the TMR as a unique energy source for synfuel (H_2) production, we have stipulated for our scoping that the dc electrical energy component Bn_{dc} of the direct convertor will be used, in the first place, to satisfy the circulating power and the auxiliary needs of the reactor itself. This means simply that the dc component of the direct convertor drives the reactor and the ancillary equipment. No other energy input is required. As can be surmised, there will be a specific value of Q at which this demand is exactly satisfied. For higher Q values, there will then be a surplus of dc electrical energy that will then be used by the thermochemical plant. For lesser values of Q, some thermal energy from the reactor blanket or from the thermal part of the direct convertor would have to be converted to electrical energy to help drive the reactor. We define Q as the fusion power/injected power.

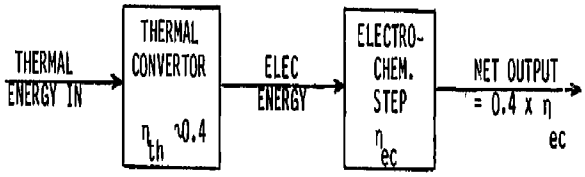

The HTGR, the Tokamak, solar energy concentrators must convert thermal energy to electrical energy at an efficiency η_{th} to drive the electrolysis step or meet other electrical demands of the thermochemical cycle.

Fig. 10A. HTGR, Tokamak or solar energy concentrator energy sources.

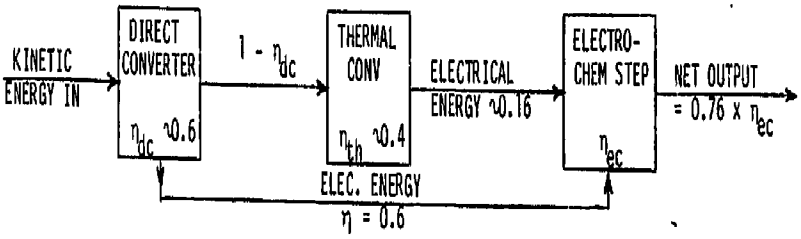

The Tandem Mirror Reactor can drive the electrolysis step directly or provide other electrical demands directly using the reactor's dc electrical output.

Fig. 10B. The Tandem Mirror Reactor energy source.

It may be seen from Fig. 11 that when the Q value is about 11-14 or higher, there begins to be a dc electrical component left over from the reactor that can be used to drive such things as electrolysis cells, pumps, motors, etc., in the synfuel plant.

Relative to the total energy that the reactor has created for synfuel purposes, the fraction that is dc tends to a limit R, where R is defined as surplus dc (expressed in units of equivalent thermal energy) divided by the total energy available to the process chemistry. Expressing surplus dc in thermal units is somewhat of an artifice but is useful in illustrating limits. This limit is indicated in Fig. 12 where we see that as Q gets larger and larger, the dc percentage of the reactor's output available for process chemistry tends to a limit of about 13% for the D-T cycle.

In Summary Then the Unique Features of the Tandem as an Energy Source for Synfuels Are as Follows:

From Figs. 11 and 12 some conclusions can be reached.

1) At a Q value of about 11-14 the TMR dc electrical output is just large enough to feed back and drive the reactor, leaving the thermal fraction of the direct convertor and the blanket thermal energy available for process chemistry.

2) As Q values exceed 11-14 there is some surplus dc electrical power available for process chemistry.

3) As Q increases the direct current electrical energy that is available for process chemistry tends to a limit of about 13% of the plant useful output.

4) The availability of this direct current electrical energy from the TMR is an asset that other energy producing machines do not have. The HTGR, the Tokamak, the LWR, the FBR -- all of these machines must go through the thermal conversion step to produce this electricity at a penalty that is directly proportional to the thermal efficiency. The TMR begins to avoid the thermal step when values of Q exceed about 11-14.

Looking to the Future - The TMR and the D-D or D-^{3}He Cycle

When we consider only the D-T fuel cycle, there is a limit for the charged particle energy out of the TMR that cannot exceed 20% of the total energy output, i.e., 3.5 Mev alphas out of the total energy of 17.6 MeV (14.1 Mev neutrons + 3.5 Mev alphas).

If a D-D fuel cycle were to be considered the picture changes significantly. With the D-D cycle it is possible to have approximately 50% of the raw energy output of the TMR in charged particle form and convertible to electricity directly. It is interesting to compare the two cycles (the D-T

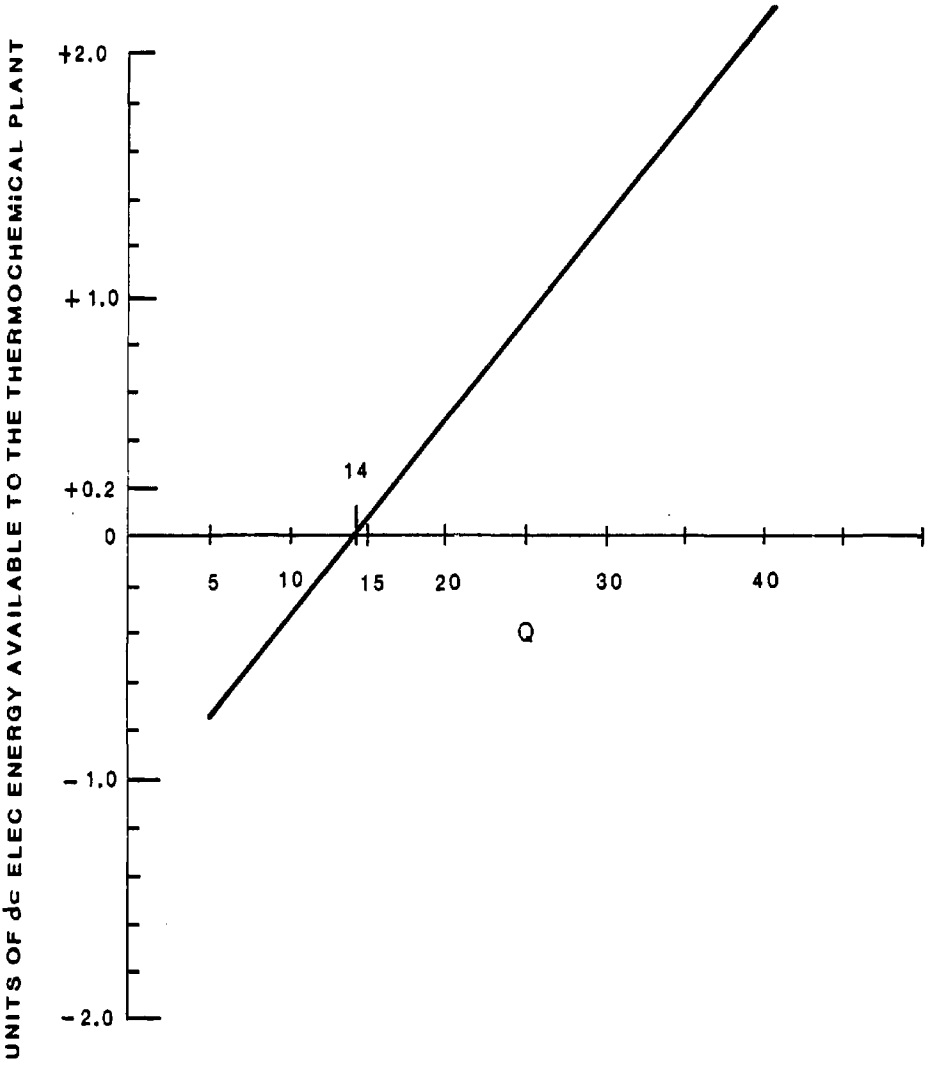

Fig. 11. Units of surplus electrical energy vs Q. Tandem Mirror Reactor.

$P_{surplus} = [P_{dc} - (P_{aux}+P_{circ})]$

$P_{nj} = 1.0$

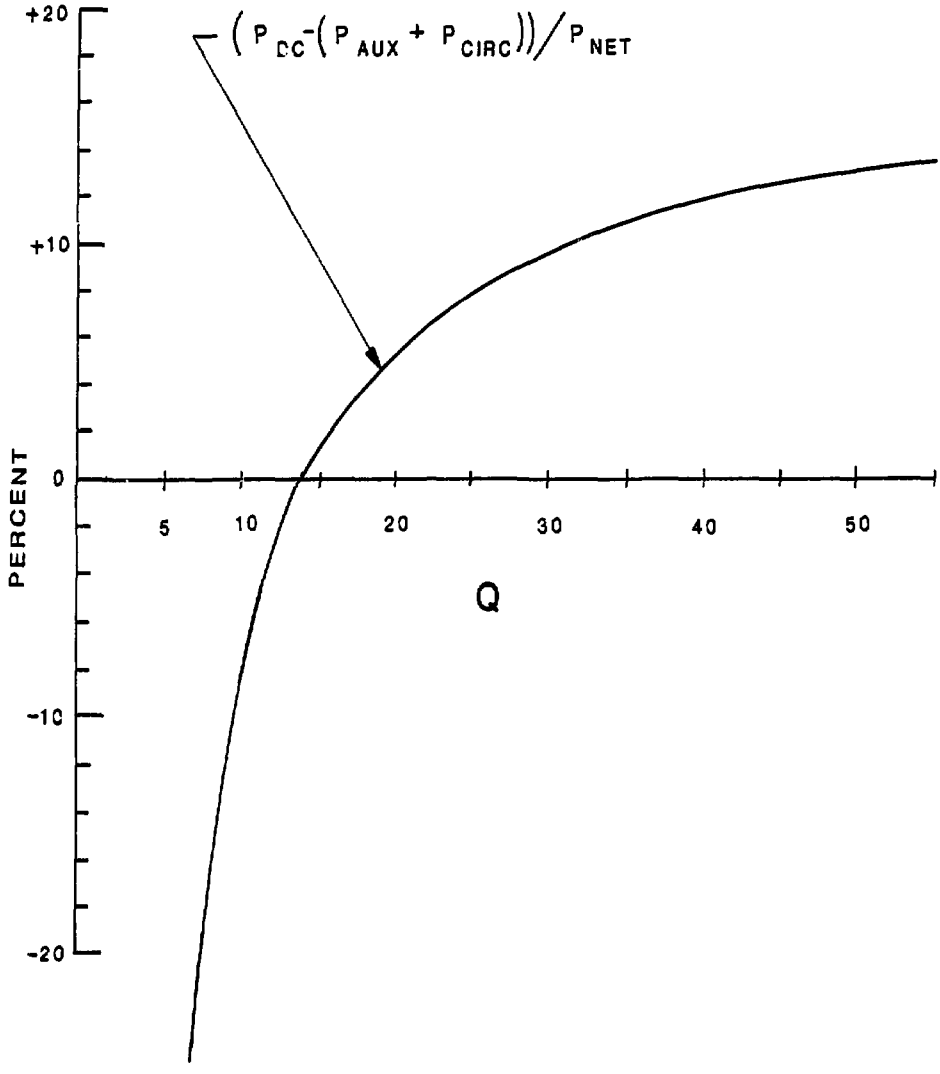

Fig. 12. Net dc power available to the process plant as a percentage of total process heat in constant units.

and the D-D) for their overall plant efficiency potential and also to compare the TMR with the Tokamak, the HTGR or a solar concentrator under these circumstances. This comparison is shown below in Fig. 13.

We are of the opinion that the D-D cycle, although difficult from a physics standpoint, may be significantly superior to D-T from an engineering/technology viewpoint. The economics may be in question because of poorer reaction cross-section. However, the environmental/ political influences and pressures that will inevitably be brought to bear on fusion's acceptability to the community cannot be ignored. The inexhaustible energy advantages and safety advantages of deuterium fuel over tritium fuel are also important and particularly interesting when coupled to the production of hydrogen.

OVERALL EFFICIENCY POTENTIAL OF DIFFERENT ENERGY SOURCES

- Tandem D-T cycle

$$\eta_{net} = 0.8\ \eta_{th} + 0.2\ \left[\eta_{dc} + (1-\eta_{dc})\,\eta_{th}\right]$$

$$\eta_{net} \simeq 0.32 + 0.146 \simeq 47\%$$

- Tandem D-D Cycle

$$\eta_{net} = 0.5\ _{th} + 0.5\left[\eta_{dc} + (1-\eta_{dc})\,\eta_{th}\right]$$

$$\eta_{net} \simeq 0.20 + 0.365 \simeq 57.5\%$$

- Tokamak D-T Cycle or D-D cycle, the HTGR or a Solar Concentrator

$$\eta_{net} = \eta_{th}$$

$$\eta_{net} = 0.40 \simeq 40\%$$

Fig. 13. Overall efficiency potential of different energy sources.

THERMAL HYDROGEN PRODUCTION

The partitioning of the TMR energy available for process chemistry must first be considered. It is convenient for structural and thermodynamic reasons to divide all of the blanket energy into two sources of supply usable for the process chemistry. The first supply source (the FWHX) is the cooled first wall zone, characterized by modest (700 K) energy levels since the first wall serves as the structural container for the fluid in the module. The second zone, the condensing vapor heat exchanger (CVHX), is where high temperature, high-quality heat (1200 K) is produced for the main part of the thermochemical processes. The direct converter thermal heat exchanger (DCHX), not shown, operates at a temperature ∿900 K. The energy distribution is approximately:

1200K CVHX ∿80-85%
700K FWHX ∿5-10%
900K DCHX ∿10%

The Thermochemical Cycles

The TMR is used as an energy source to produce fuel (H_2) via three candidate thermochemical cycles.

- Sulfur-Iodine Cycles: (General Atomic)

$$2\ H_2O + SO_2 + I_2 \xrightarrow{\text{AQUEOUS}} H_2SO_4 + 2\ HI_x$$

$$2\ HI_x \xrightarrow{< 573K} x\ I_2 + H_2$$

$$H_2SO_4 \xrightarrow{< 1144K} H_2O + SO_2 + 1/2\ O_2$$

- Sulfur Cycle (part electrochemical): (Westinghouse)

$$2\ H_2O + SO_2 \xrightarrow[\text{ELECTROLYSIS}]{\text{AQUEOUS}} H_2 + H_2SO_4$$

$$H_2SO_4 \xrightarrow{\text{HIGH T}} H_2O + SO_2 + 1/2\ O_2$$

o Sulfur-Bromine Cycle (part electrochemical): (Ispra)

$$2\ H_2O + SO_2 + Br_2 \xrightarrow[320\text{-}370K]{\text{AQUEOUS}} H_2SO_4 + 2\ HBr$$

$$2\ HBr \xrightarrow[\text{ELECTROLYSIS}]{\text{AQUEOUS}} Br_2 + H_2$$

$$H_2SO_4 \xrightarrow{1000\text{-}1100K} H_2O + SO_2 + 1/2\ O_2$$

These three cycles have been demonstrated in closed loops on a laboratory scale.

The requirement for energy, thermal and electrical, for these three cycles are illustrated in Table 2.

The flow concept for coupling the TMR to the G.A. cycle involves either liquid sodium or helium from the condensing vapor heat exchanger in the cauldron blanket vapor dome to the SO_3 decomposer heat exchanger as discussed earlier[8] as Concept #1, Fig. 14.

The SO_3 decomposer is the critical process unit in nearly all of the viable thermochemical plants that produce H_2. These plants can be driven by high-temperature gas cooled reactors, solar collectors or fusion reactors with sodium,potassium, or helium. These heat transfer fluids supply the large heat demand of the SO_3 decomposer by means of heat exhangers that are an integral part of the decomposer. Catalysts are required in this decomposer in order to keep the temperature required down to reasonable levels of 1073 to 1173K. The cost of these catalytic decomposers heated by internal heat exchangers appears not to be too large in order to keep the plant cost competitive with other H_2 production technologies.

Table 2

ELECTRICAL AND THERMAL REQUIREMENTS FOR VARIOUS CYCLES

BASED ON HTGR HEAT SOURCES

Thermo-Chemical Cycle	Thermal Eff.	Process Heat		Thermal Energy Used Generate Electricity Or Shaft Work	
		High Temp	Intermed. Temp	Electrolytic Demand	Process Shaft Work
General Atomic Sulfur-Iodine Cycle	47%	24% 1250 K	51% 843 K	0	25%
Westinghouse Sulfur-cycle Cycle	47%	23% 1280 K	20% 1108 K	57%	0
Ispra Mark-13 Cycle	46%	27% 1083 K	52% below 773 K	21%	0

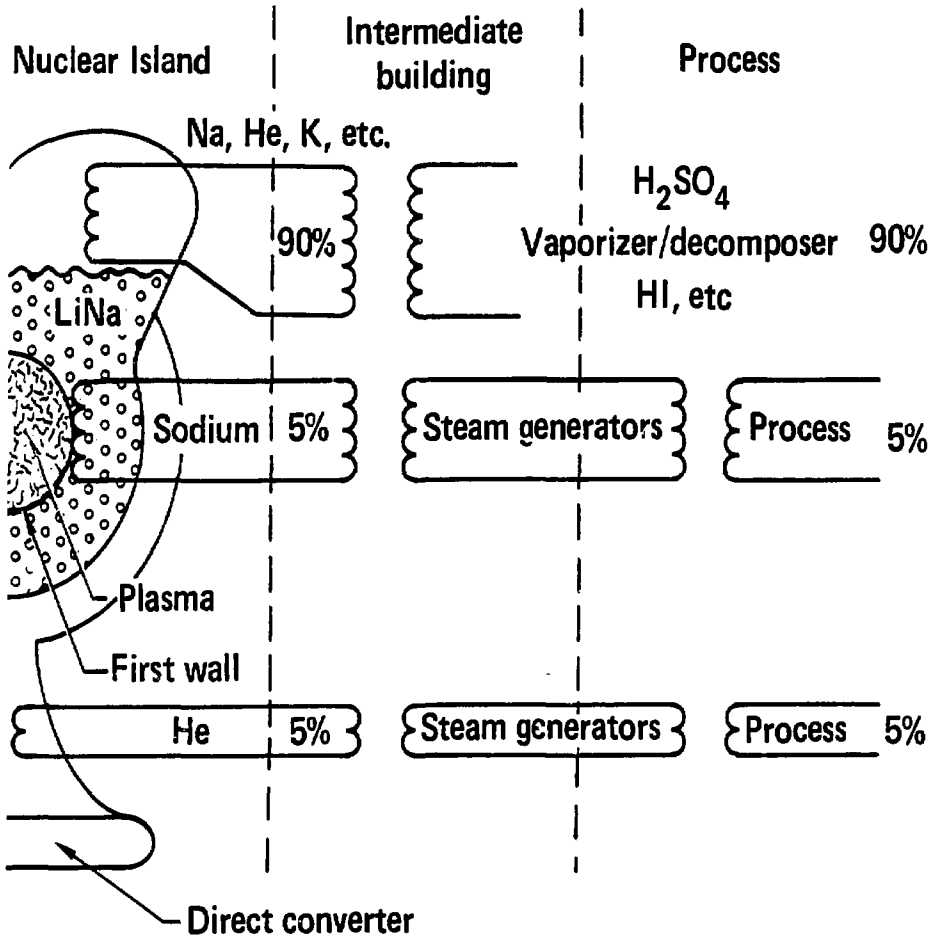

Fig. 14. Concept #1 interface. Coupling the G.A. Cycle to the TMR.

The background chemistry on the SO_3 decomposition reaction includes work at Westinghouse,[9] the Nuclear Research Centre in Julich, Germany,[10] General Atomic in San Diego,[11-13] and the Joint Research Centre at Ispra, Italy.[14] The theoretical effect of temperature and pressure on the SO_3/SO_2 equilibrium in the presence of water vapor is available.[13] At around 5 atmospheres reactor exit total pressure and ~1050K, the fraction SO_3 converted to SO_2 is around 55%. We have picked ~5 atm and ~1050K for the SO_3 decomposer chemistry with the aim of alleviating problems with catalysts and reducing materials' problems in the decomposer and in the TMR blanket. This compares to G.A.'s 74% conversion at 1144K.

A sensitivity study was done and was reported earlier, showing the tradeoff between equipment size and this level of SO_3 decomposition selected as a design basis. In reducing the conversion from G.A.'s 74% to our 55% the volumetric vapor load only increases 7.4%, which has a very small impact on the size of the expensive multi-effect evaporator train.

CHEMICAL KINETICS

Now that we have established the flowsheet and material balance, we need to turn to the chemical kinetics of the SO_3 decomposition.[9-14] In comparing the current experimental and theoretical understanding,[9-14] we will show that there is a substantial agreement between the findings of G.A.,[11,12] JRC-Ispra,[14] and Westinghouse[9] for catalytic bed residence times.

Perhaps the most detailed studies of SO_3 reaction kinetics with varying residence time were done on the Fe_2O_3 catalyzed system by the Commission of the European Communities, JRC-Ispra Establishment, Italy, and reported recently.[14] Their results are reproduced in Fig. 15. They show percent conversion versus residence time defined as the catalyst volume divided by the volumetric flow at 273K and 1 atm.

For economic reasons we want to select a low residence time, but consistent with high conversion. Ispra selected around 1 s at 64% conversion. Although residence times down to around 0.7 s appear feasible from Fig. 15, the steepness of the curve causes the reactor to be unstable. Unfortunately, in their work they only examined Fe_2O_3 in this detail and not the more active platinum-based catalysts. Much of their catalyst work remains IEA restricted.

We therefore turn to the work of G.A., where a variety of catalysts has been studied,[11,12] but in less detail. G.A. carries out their studies using a different definition of residence time with the volumetric flow based on process temperature and pressure instead of STP, i.e.:

$$\tau = \frac{\text{vol. cat. bed voids, } m^3}{\text{vol. flow at T,P, } m^3/s} \quad . \qquad (2)$$

For comparison, a residence time using Ispra's definition would be comparable to a 20% lower residence defined as in equation (2) above (at 1050K and 6.5 atm).

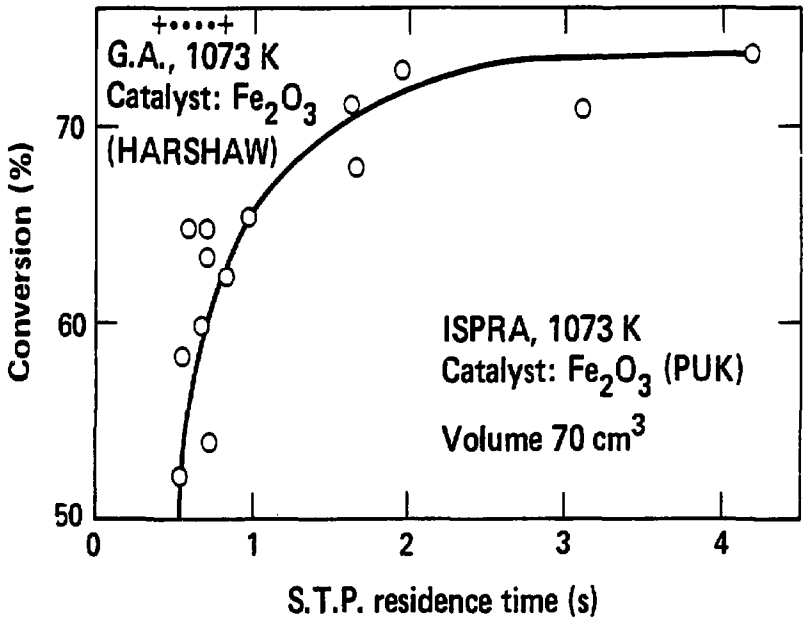

Fig. 15. Hydrogen production by decomposition of 96% H_2SO_4.

In G.A.'s studies[11,12] the residence time was varied from 0.2 s on up, and catalysts[11,12] such as Fe_2O_3, CuO, and Pt appeared to be attractive for our proposed conditions of ~5 atm and 1050K without showing any decline in performance down to 0.2 s. In other words, their conversion performance remained high on a flat portion of the conversion - residence time plot down to 0.2 s as shown in Fig. 15. We conclude that the G.A. Fe_2O_3 catalyst is far better than Ispra's Fe_2O_3 catalyst.

For the purpose of this design we have selected 0.5 s as the residence time for the SO_3 decomposer as being safely on the high, flat portion of the conversion - residence time plot based on G.A.'s work.[11,12] Without the use of catalysts G.A. has shown[11] that the conversion of SO_3 to SO_2 would be only 3% at 1050K and that another 200K would be required to achieve 95% at 1250K. Thus, a complete elimination of the catalyst would be possible at 1250K. We have reviewed carefully the G.A. work at 1050K[11,12] and found that we could eliminate the need for the expensive platinum catalysts by substituting the much cheaper CuO (Cu-0803T) or Fe_2O_3 (Fe-0301T) catalysts available from Harshaw Chemical.* These latter catalysts perform nearly identically, however, they are both deactivated by a sulfation reaction involving the substrate on which the active metal oxide is placed. We have selected CuO as preferable on the basis of a deactivation temperature around 950K, as compared to Fe_2O_3 at 1000K.[12] This still represents some risk in case of temperature excursions in the Decomposer Reactor. Consequently, we have selected CuO, but with Pt as a backup.

THE IMPORTANCE OF CATALYST GEOMETRY

We have reviewed the experimental apparatus of Norman, et al., at G.A.[15] and found the laboratory reactor to be a basic plug flow unit with the catalyst bed contained in a quartz tube 1.8 cm I.D. and 5 cm long. Catalyst pellets as short cylinders, 3.13 mm in diameter and length were used. We estimate from early packing studies of pellets[16] in their Fig. B-13 that for an effective spherical diameter of 4.01 mm these pellets will pack into a 1.8 cm I.D. cylindrical vessel with a void fraction of 0.39 including the vessel wall void defect. For larger commercial vessels, with less of a wall effect, void fractions of ~0.35 can be expected.

In this paper we examine some of the chemical engineering tradeoffs resulting from decomposer reactors of a fluidized bed, packed bed, and heatpipe/catalytic cartridge geometry.

*Reference to a company or product name does not imply approval or recommendation of the product by the University of California or the U.S. Department of Energy to the exclusion of others that may be suitable.

Packing information and the definition of the residence time, τ, used by G.A.[11,12] as in equation (2) above can be used to estimate the catalyst requirements for a fluidized decomposer. The decomposer maximum total volumetric flow (including H_2O, SO_3 and recycle) that would be possible for our plant driven by a 5,000 MW_t TMR with a process heat demand of 608.85 kJ/gmol H_2[17,18] can, therefore, be calculated as 437 m^3/s at 1050K and 6.5 atm. The latter pressure was selected as an average of the SO_3 decomposer inlet and outlet conditions. Now from equation (2) we can estimate first the volume of required catalyst at 560 m^3, assuming the same catalyst geometry as used in the experimental work of G.A.

We can now estimate the labor and metal capital costs for both CuO and platinum-based catalysts from a recent quotation from Englehard.[19] CuO placed on an alumina substrate would represent a labor and capital cost of around $4.15 million. Platinum placed on titania at 2% Pt (considered the lower limit of commercial experience) would represent a labor cost of $5.33 million and an initial platinum capital cost of $107 million. We have reviewed the G.A. literature[11,12] and found that the catalyst performance remains equally effective down to 0.08% Pt and perhaps even lower. This very low platinum level would reduce the platinum metal capital cost down to $4.27 million which is deemed acceptable. We should add here that for large utility companies that might operate such large plants, they might already own or participate in a "platinum pool." The pool concept is widely used today and provides a "loan" of platinum for use on catalysts, with the notion that the platinum is not consumed but can be recycled back for credit and redeposition on a new substrate for the manufacture of fresh catalyst.

In our estimates for the catalyst volume of 560 m^3 we assumed that the volume fraction of the catalyst substrate which is active is the same for the G.A. pellet catalyst and our smaller fluidized bed spherical catalysts. We know[20] this to be quite conservative as shown in Fig. 16. The catalyst is really active only to a depth of 150 μm and has no activity beyond 250 μm.[20] If we allow for this reduction in the inert substrate volume at the center of the catalyst in scaling from the G.A. pellet to a smaller size sphere, the catalyst volume requirement would be markedly reduced. A larger reduction is obtained if the entire catalyst sphere is considered active right down to the center. With activity falling to zero around a radius depth of 0.25 mm (250 μm), a small 0.5 mm diameter catalyst would be ideal.

We examined the consequence of a 0.5 mm catalyst and found a 2.5 to 7-fold reduction in catalyst volume requirements and that the decomposer volume could be reduced in size a factor of 2 or 3; however, the temperature gradients all increased so the overall ΔT increased from 22°C to around 60°C for a sodium driven unit and 30°C to 70°C for a helium driven unit. This could be countered by doubling or tripling the number of heat exchanger tubes, with an unavoidable increase in cost associated with higher complexity. So the benefits of a catalyst requirement reduction are difficult to capitalize on without attendant increases in ΔT or cost. But, this is a tradeoff that should be kept in mind in future estimates of overall plant economics.

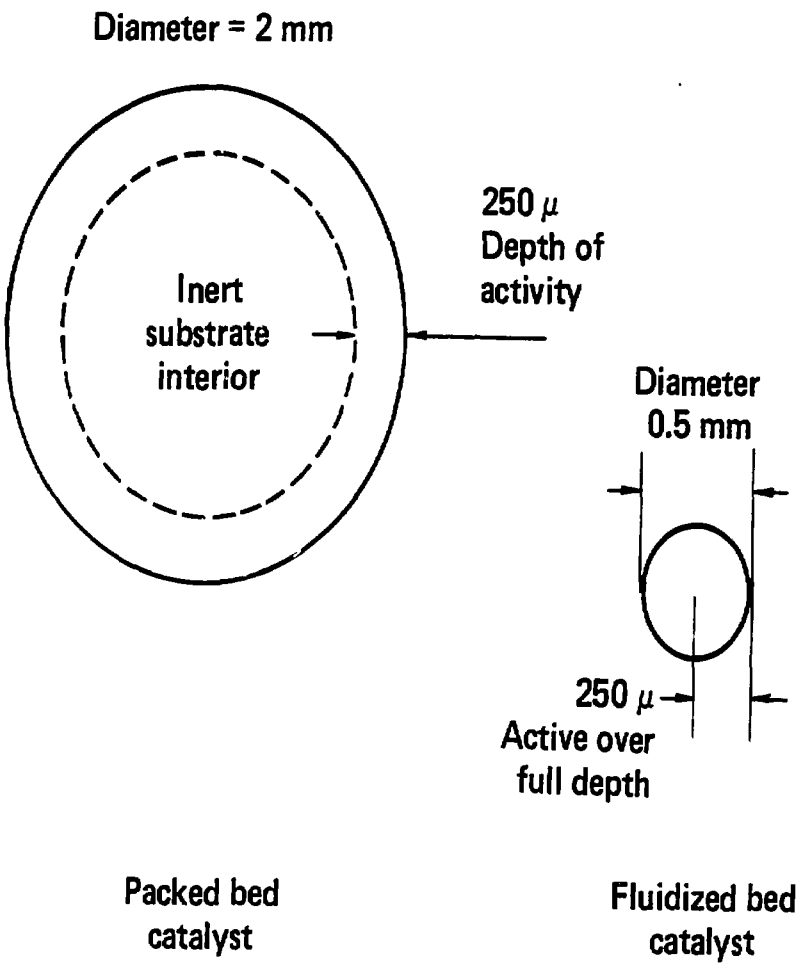

Fig. 16. Catalyst geometry and contrast between packed bed and fluidized bed catalysts.

A FLUIDIZED BED SO_3 DECOMPOSER DESIGN

The design of chemical reactors with fast kinetics and large associated heat effects is one of the toughest problems in the chemical process industries.[21] We have spent a substantial effort examining different types of chemical reactors to try to establish a design of least cost and greatest simplicity. The choice is made more difficult since the detailed SO_3 decomposition kinetic rate law is not known. Experimental and analytical difficulties for this very fast reaction have greatly hindered its determination.[11,12] Therefore, we cannot determine such choices as the advantages of recycle, back mixing, residence time distribution, secondary addition, etc. Kinetics should be planned in any future work.

The analysis[8] for the first obvious choice, a plug-flow, packed bed reactor, shows this choice not to be feasible because of extremely large temperature gradients (i.e., 68°C) between the internal heat exchanger fluid supplying the heat to this highly endothermic reaction and the packed bed of catalysts. Furthermore, large radial temperature gradients appear within the bed between the internal heat exchanger tube elements.

This problem of supplying the requisite heat into the decomposer has forced us to fluidized bed designs.[22] Using a catalyst particle size of 0.5 mm and a catalyst density[19] of 0.96 Mg/m^3 and a gas viscosity[16] of 0.04 g/m-s, the minimum fluidization velocity, U_{mf}, can be estimated[21] as $U_{mf} = 0.0428$ m/s.

This velocity is well below the entrainment velocity $U_t = 3.67$ m/s. We must operate the fluidized catalytic decomposer between these limits. We have selected the velocity to be $U_f = 1$ m/s.

At this velocity we can calculate the bed expansion[22] to be $\varepsilon = 0.8$. Consequently, the new bed volume will be 1627 m^3 total, which can be broken up into 7 beds of reasonable but large size: 8 m high by 6 m in diameter.

For such decomposer vessels we find the particle Reynolds number will range from 34 to 82. We estimate a $-\Delta P = 1.66$ atm. We have also allowed about 1 atm pressure drop across the distributor plate; thus $-\Delta P = 2.6$ atm total.

The pumping work can now be estimated for fluidizing this bed of catalyst. For 7 beds of 6 m in diameter the volumetric flow rate is 198 m^3/s and the work needed at this ΔP would be 51.4 MW_e. We indicate this as electrical work although it is nearly equivalent to shaft work. This work requirement is for a basis 5,000 MW_t reactor rating. For a 3,000 MW_t basis, 4 catalytic decomposers would be used, and for 2,000 MW_t, 3 decomposers, and for 1,000 MW_t, 1 decomposer. A better way of expressing the pumping work is per unit H_2 production; this is 6.3 kJ/gmol H_2, which is independent of scale. We consider this to be an attractively small value.

Heat Transfer Aspects of the SO_3 Decomposer

We indicated earlier that the problem of supplying the endothermic heat requirements is a serious one; consequently, we now make a better estimate of the significant thermal gradients within the decomposer.

We first examine the catalyst surface to assess the ΔT there. We estimate[23] the fluidized bed parameters as $\varepsilon = 0.8$, $\varepsilon_b = 0.05$, and turbulence level $Z_t = 0.25$. The Frossling group[23] is found to be Fs = 0.65 and the Nusselt number ranges from 11.6 to 16.9, which corresponds to a heat transfer coefficient, h, ranging from h = 1183 to 1724 kcal/h-m^2 catalyst. The total catalyst external surface area for 7 beds is 3.87×10^6 m^2. With an endothermic reaction ΔH_R = +23.59 kcal/gmol SO_3 and 1.561 gmol SO_3/gmol H_2 in the decomposer feed, we calculate: $\Delta T = 0.24°C$.

The available experimental literature[22] indicates that in fluidized beds when the gas-solid heat transfer is good, as in our case with ΔT = 0.24°C, the particles and the gas are at thermal equilibrium and there are never significant ΔT's within the fluidized bed itself. Instead, the heat transfer from the fluidized bed to the heat exchanger surface is always controlling.[22] And, so it is in our case.

The heat transfer resistance occurs across a thin film between the fluidized bed and the surface of the heat exchanger vertical tubes. For this case the Wender and Cooper correlation applies.[22] This correlation predicts a wall Nusselt number of 24.23 and, thus, a heat transfer coefficient, h_w, of 673 cal/m^2-s-°C.

We set the maximum number of tubes in the decomposer by limiting their volume fraction to 10% and their tube diameter to 2 cm O.D. Since the expanded bed volume is 1583 m^3, the tube volume cannot exceed 158.3 m^3. This corresponds to a total of 63,000 tubes distributed between the 7 decomposer units, or 9,000 tubes per decomposer placed on a hex pitch of 6 cm. These tubes must provide 4.29×10^4 kcal/s for each decomposer unit. Combining this heat requirement, the tube area of 4523 m^2, and h, we obtain that this film ΔT = 14°C. This is high, but acceptable for fluidized beds.

Next, we examine the sodium heat transfer fluid within these tubes. First, we require that the sodium not decrease in temperature more than 100°C over its course through these tubes. For liquid sodium with a $C_p = 0.32$ cal/g-°C, this is equivalent to specifying the mass flow at 1.516×10^3 kg/s for each bed. We can use the Martinelli correlation[24] which is specifically applicable to liquid metals. For sodium around 1050K, with a thermal conductivity, k = 19 cal/s-m-°C, a viscosity of $\mu = 0.2$ g/m-s, and density of 0.8 Mg/m^3, we estimate the Reynolds number at Re = 50,000 and Prandtl number at Pr = 0.0037. Thus, the ΔT = 0.2°C, which is very low and quite acceptable.

We can next estimate the sodium pumping work through 10 m long tubes from the friction factor of f = 0.02,[16] ΔP = 0.02 atm, and volumetric flow of 13 m^3/s for all 7 beds, or 0.02 MW_e for a 5,000 MW_t reactor or 2.92 J/gmol H_2 for any size reactor.

We have also estimated the ΔT across the 3 mm tube wall to be 6°C for Incoloy-800H to complete the decomposer vessel heat transfer analysis. We have combined all of these ΔT's in a schematic for the final decomposer configuration shown in Fig. 17. The overall ΔT between liquid sodium and the catalyst center is about 22°C. The liquid sodium feed temperature desirable would be around 1125K at 7 atm. We selected the SO_3 range in temperature in Fig. 16 from 1003 to 1103K so that the average will remain at ~1050K. The yield is taken at 55% as if an isothermal condition of 1050K was maintained. Without more detailed kinetic studies on SO_3 decomposition, little more is possible.

We looked at the possibility of placing a He gap of 0.6 mm in a duplex tube design to provide additional safety isolation between the sodium and the O_2-containing process stream. We found that the ΔT across this gap would be 78°C -- unacceptably increasing the blanket temperature. This problem was a further motivation for examining He as the heat transfer fluid later in this paper.

Preliminary Costs

We have also estimated the mass of these tubes (3 mm wall) and vessels (2 cm wall) to be 952 Mg and 211 Mg respectively. We find for the Incoloy-800H tubing, unit costs of around $24/kg, which cost out around $25 million. Incoloy-800H vessels would cost around $2.5 million. CuO or platinum catalysts would add $5.33 million for metal deposition labor and for Pt, $4.27 million for inventory at 0.05% Pt. So our upper limit for an Incoloy-800H decomposer cost would be around $50 million, allowing around 40% for supports, ladders, instrumentation, and supporting hardware. Using a 20 year plant life, a stream factor of 85%, an interest rate of 12% and a zero equity, a rough H_2 product cost of 12¢/GJ attributed to the decomposer is estimated. If the fusion plant is around $2 billion or $4/GJ, the material costs for the SO_3 decomposer appear quite low in comparison.

A parametric study was done on varying the decomposer temperature. The mass balances were done for 100K higher and 100K lower temperature. The flows vessel sizes and costs, and pumping power are shown in Table 3. There is a clear tradeoff between lower temperature and increased evaporator and decomposer vessel size, pumping power, and costs.

TABLE 3

A PARAMETRIC STUDY ON VARYING DECOMPOSER TEMPERATURE

	DECOMPOSER TEMPERATURE		
	1144 K	1050 K	950 K
SO_3 Conversion, $SO_3 \rightarrow SO_2$	0.735	0.55	0.29
Total Molar Flow in Evaporators, gmols/s	27,530	35,560	61,292
Volumetric Flow in Evaporators, m^3/s	397	437	735
Volume Decomposer Catalyst, m	466	560	942
Catalyst cost, Pt Labor, M$	4.44	5.33	8.9
0.05% Pt, Pt Inventory, M$	3.70	4.27	7.4
Number of Catalytic Decomposers in Use	6	7	12
Fluidization Pumping Power, kJ/gmol H	5.5	6.3	10.9
Liquid Sodium Pumping Power, J/gmol H	2.5	2.9	5.0
Decomposer Installed Costs Incoloy-800, M$	45	50	90

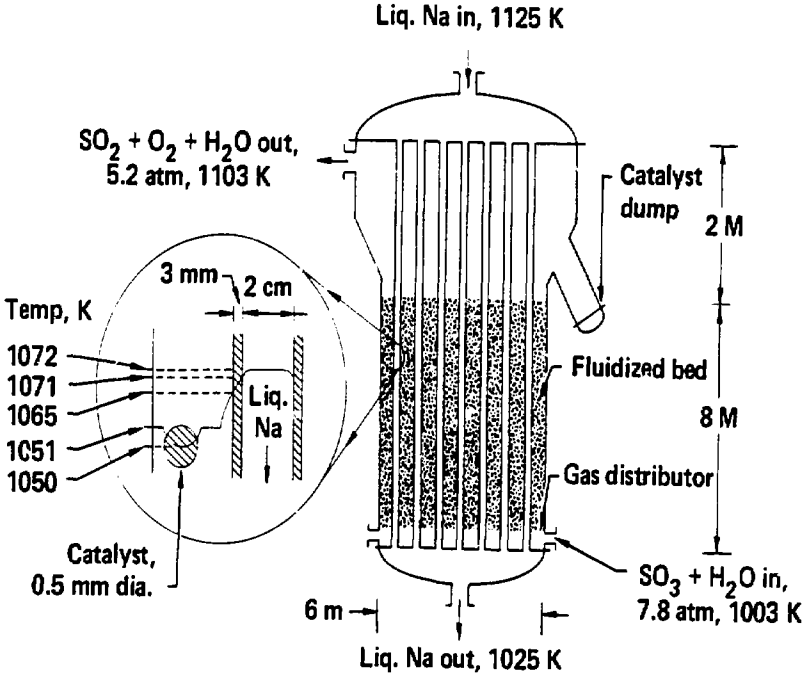

Fig. 17. Fluidized bed catalytic SO_3 decomposer.

We also did a parametric study on varying the sodium flow rate through the tubes. Increasing the flow from 1516 kg/s per bed to 13,400 kg/s per bed dropped the sodium ΔT across the SO_3 decomposer from 100°C to 10°C. Under these conditions in order to keep the catalyst at 1050K, the sodium feed temperature could be dropped from 1125K as in Fig. 16 down to 1082K. This is a drop of 43°C on the temperature requirement that must be provided by the fusion blanket, thus easing the alloy and safety problems in the blanket design. This is traded off with the added size of the transport piping and condensing vapor heat exchanger within the Cauldron blanket module.

The choice of material[25] for a sodium-driven SO_3 decomposer would involve on the sodium side a 0.5 mm steel clad (Fe, 2-1/4% Cr, 1% Mo) on the inside of the Incoloy 800H heat exchanger tubes. On the SO_3 process side, the Incoloy 800H would be coated with an aluminide layer, 100 μm or so thick.

Helium as an Increased Safety Option

We repeated the above design procedure while replacing the liquid sodium by helium as the heat transfer medium to carry the blanket heat out to the H_2 thermochemical plant. We illustrate with an example, which we believe to be a reasonable case and we expect to do a more detailed optimization on the combined system later in the year. We used a ΔT = 50°C across the SO_3 decomposer and operated helium at 30 atm total pressure in order to minimize the stresses on the SO_3 decomposer internal tubes. The helium mass flow required was 1198 kg/s per bed or 120 m/s velocity for a decomposer with 18,000 tubes per bed (twice the number and twice the cost as in the sodium unit). The film ΔT for helium to the inside of these tubes was 18°C, thus raising the overall ΔT to about 30°C, very little above the sodium unit's 22°C. The pressure drop was 1.0 atm across the decomposer, creating a pumping power of 110 MW_t (40 MW_e) or 8.1 kJ/gmol H_2 for all 7 beds. Thus, from the decomposer standpoint, He is a viable candidate and achieves greatly improved safety isolation between the O_2-containing process stream and the blanket Li-Na pool. High helium pressures (i.e., 60 atm) will allow us to reduce the tubes back to 9,000, and will reduce pumping power to 60 MW_t; but the added pressure will force us to double the tube thickness from 3 mm to about 6 mm. The cost would nearly double. The materials we have selected for the He-driven SO_3 decomposer would involve Incoloy-800H at 2 mm thick wall, 20 mm diameter O.D., under our conditions of 30 atm. the stress level would be around 7.15 MPa (1100 psi), offering a safety factor of 2 over the 1% creep, 10,000 hours value of 13 MPa (2000 psi) $\pm$ 50% (quoted in Section 8 of Reference 20).

A rough cost analysis was done on this attractive helium alternate case of a 30 atm, 120,000 tubes of Incoloy-800H, 7-bed decomposer operating with an overall ΔT = 50°C. The basic fabricated tube cost at $24/kg would be $46 million. This roughly doubles the decomposer cost to 11¢/GJ, which is acceptable; however, the transport piping must be designed to handle the added pressure. In the case of sodium coolant at 1.5 atm, the piping could be inexpensive single wall, 5 to 10 mm thick, placed in a safety channel -- at a rough total cost of around $13 million or 1.5¢/GJ. A single wall helium piping wall thickness[25] would be 150 mm at a temperature of 1100K and would

cost around $250 million -- this appears unacceptable. A pressure balanced hot wall concept, with a 1.2 cm thick stagnant helium layer, would allow the outside wall to cool to 870K (i.e., 200K cooler). This would allow a stress up to 1860 MPa (27,000 psi). Using the criteria of 1% creep in the 20 year life, we would use a 33 mm (1.28 inch) wall at a cost of $50 million or 12¢/GJ, which is acceptable.

We find that the key factor that forces the cost upward is the requirement to supply heat to the catalytic surfaces where the endothermic SO_3 reaction occurs. Transferring heat from in-bed heat exchangers to packed beds of catalysts is very inefficient and requires large temperature differences and costly, high heat transfer media flow rates. Fluidization of the bed of catalysts helps greatly in reducing the temperature differences between the heat transfer fluid and the catalyst surface. However, it takes substantial pumping power to supply enough energy to the SO_3-containing gas in order to fluidize the bed.

A new concept that we are studying of a catalyst cartridge surrounding a heat pipe which is driven by the heat source, corrects these serious problems. No dangerous sodium or potassium heat transfer fluids need be used, no large temperature differences are required between the heat source and the catalyst surface, no large heat transfer fluid flow rates are required, no high pressure helium is necessary, and a triply contained safety system results with a cover gas to monitor leaks and sweep out any tritium that permeates through the wall.

Axial-Flow Cartridge

Two preliminary versions of the cartridge concept have been developed. The first version is shown in Fig. 18. The cartridge is flange-mounted to a manifold where helium sweep gas and process (SO_3) gas can be individually flowed. The gas-buffered heat pipe transports the heat from the heat source out into the catalytic cartridge reactor where the SO_3 decomposition occurs at 1050K. The heat pipe concentrates the permeated tritium to the right-hand end where it is removed through a niobium window. Any tritium which permeates radially out of the heat pipe is swept to the right by the helium sweep gas and is removed before it can contaminate the $SO_2 + O_2$.

The catalytic surface is kept hot at 1050K by the heat pipe and SO_3 flows over its surface and is converted to $SO_2 + O_2$. These gases flow in the annular space where the inside surface is coated with a catalyst and possibly the outside surface could be coated as well. This entire cartridge can be removed for catalyst regeneration or reactivation. The catalyst may be precious metal or metal oxide, but a high quality thermal contact is not required. The metal alloy could be Incoloy-800H in order to resist the corrosive SO_2.

The catalyst coating on the surface can be about 250 μm thick, as discussed earlier and therefore can be fully active to the minimum volume of 80 m^3, since very little of the substrate will be inactive. For heat pipes of 1 cm diameter and a condensing region of 2 m in length, this 80 m^3

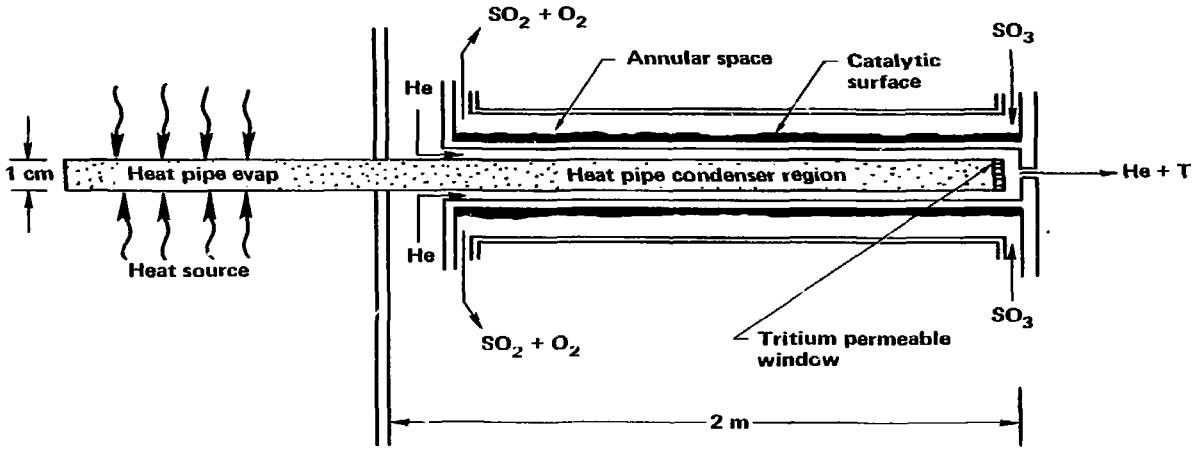

Fig. 18 Axial-flow catalytic cartridge concept.

catalyst volume can be provided with 637,000 cartridges. A single Cauldron blanket module, will allow a 1.5 m x 1.5 m area in the vapor dome to be penetrated with 12,250 heat pipe-catalytic cartridge tubes in an hexagonal array at a 12 mm pitch. This would use 26 module pairs or about 18% of the total complement of 150 module pairs. If the heat pipes were fabricated from Incoloy-800H, the fabricated cost would be around 16.7 million dollars for 1/2 mm wall or 33 million dollars for 1 mm wall. A shell surrounding the catalyst, as shown in Fig. 18, would guarantee the axial flow pattern over the catalyst (at a cost of 27.8 million), but may not be required when the tubes are placed on a hex array with a 12 mm pitch. In either case a flange-mounted distributing manifold would be required to distribute the gas at the top of the base of the cartridge.

Now let's examine the performance of this design concept. The first area of concern is the temperature drop across the 1/2 mm He gap. We estimated that for He with a thermal conductivity[26] of 0.379 J/m-s-°C and a density of 0.443 kg/m^3 at 10 atm and 1100K, that the endothermic heat demand of around 1260 MJ/s could be supplied with a drop of 69°C. This ΔT might be halved by using a grooved passage-way for the He instead of the annulus shown in the figure. We also checked to see if any radiation transfer would help, but concluded that a ΔT of 69°C at 1170K was too weak of a driving force to be significant.

The pressure drop and pumping power for the He sweep through the gap at even 1 m/s was under 0.01 atm and a few kilowatts. Since we have no actual experimental data on the tritium-concentrating capabilities of the heat pipes, we could not quantitatively estimate the permeation rate out into the He sweep along the annular gap. Since the system was designed to release the majority of its tritium at the high permeability window at the tip, we feel the permeation into the He sweep will be so low that very slow He rates, well under 0.1 m/s will be practical. In practice we could set the He sweep so that the tritium contamination into the $SO_2 + O_2$ is completely acceptable from a safety and maintenance standpoint.

We also estimated the thermal resistance within the catalyst alumina support with a thermal conductivity of 1.3 J/m-s-°C. We found that the required heat flux could be met with a ΔT drop of only 10°C.

In this design we have presumed that the SO_3 process stream enters the catalyst cartridge at 1050K and that the decomposer need not supply the sensible heat to raise the SO_3 from 800K to 1050K. This sensible heat load would add 727 MJ/s to the 1260 MJ/s endothermic heat of reaction and decrease the catalyst efficiency substantially. Consequently, we have designed a preheater to this catalyst cartridge to supply the sensible heat. The preheater would use 26 module pairs in the same configuration as shown in Fig. 18 but without any catalytic surfaces. The flow annulus could be set at a 0.5 mm gap with a velocity of 44 m/s (10% of the speed of sound) and a Reynolds number of 1 x 10^4. This would produce a film drop of 47°C. The pressure drop would be small at 0.06 atm.

Cross-Flow Cartridge

The cross-flow catalyst cartridge is the second version of the concept presented above, where an improved performance can be achieved and at a reduced capital cost. This design concept is shown in Fig. 19. The process gases flow across the catalyst-coated tubes instead of axially, as in Fig. 18. This design allows the process chamber to be a single modular unit, hermetically sealed from the He and the heat pipe. The catalyst coating for ease of deposition can cover all of the interior surfaces of this hermetically sealed process unit. These are clear mechanical advantages and there is a reduction in materials costs as well.

There are also significant heat transfer advantages as well. The cross flow around the 1 cm diameter tubes is more effective (i.e., higher Reynolds and Nusselt number at a lower process velocity) owing to reformation and growth of the boundary layer and the separation and wake formation aft of the cylinder. These wakes provide turbulence which enhances the heat transfer. At 16.6 m/s process velocity the Reynolds number is 1.78×10^4 and the Nusselt number is 130 for tubes on a hex pitch of 12.5 mm in 22 module pairs. This heat transfer prediction is based on an extensive experimental study[27] of staggered tubes in cross flow and we believe it is reliable.

We have examined the impact of this change in design on the mass transfer rate from the bulk of the SO_3 process stream to the catalyst surface. At our process conditions we estimate the binary diffusivity, $\mathcal{D}$, of SO_3 in this process stream to be 0.58×10^{-4} m^2/s. We use the heat and mass transfer analogy to translate the cross-flow heat transfer correlation[27] to mass transfer to arrive at a Sherwood number, $Sh = kgd/\mathcal{D}$, of 75.6 and thus a mass transfer coefficient, k_g, of 0.44 m/s. For a flux of SO_3 of 18,000 gmol/s or 0.75 gmol/m^2-s at about 0.5 mole fraction, we predict a concentration film drop of 0.02 mole fraction across the concentration boundary layer. Since the Schmidt number, $\nu/\mathcal{D}$, is 0.16, the concentration layer is significantly thinner than either the momentum or thermal layer and therefore offers less resistance. In addition, this analysis neglects the effect of chemical reaction on the concentration boundary layer, which has the effect to thin it even further. So from a mass transfer standpoint, the concept appears sound.

Comparison of the Two Cartridge Concepts

At this point we have several options: We could separate the SO_3 preheater from the catalyst cartridge as follows. The heat pipe would operate around 1120K. The preheater could use 22 module pairs with a helium gap ΔT of 39.7°C and a process film drop of 24.7°C. The cost of this preheater would be around $16.7 million for the unit hardware and a $5.33 million for the catalyst manufacture and deposition and $4.27 million for platinum inventory. About 20% should be added for additional hardware and instrumentation. Thus, the replacement cost would be around $46 million for the total system.

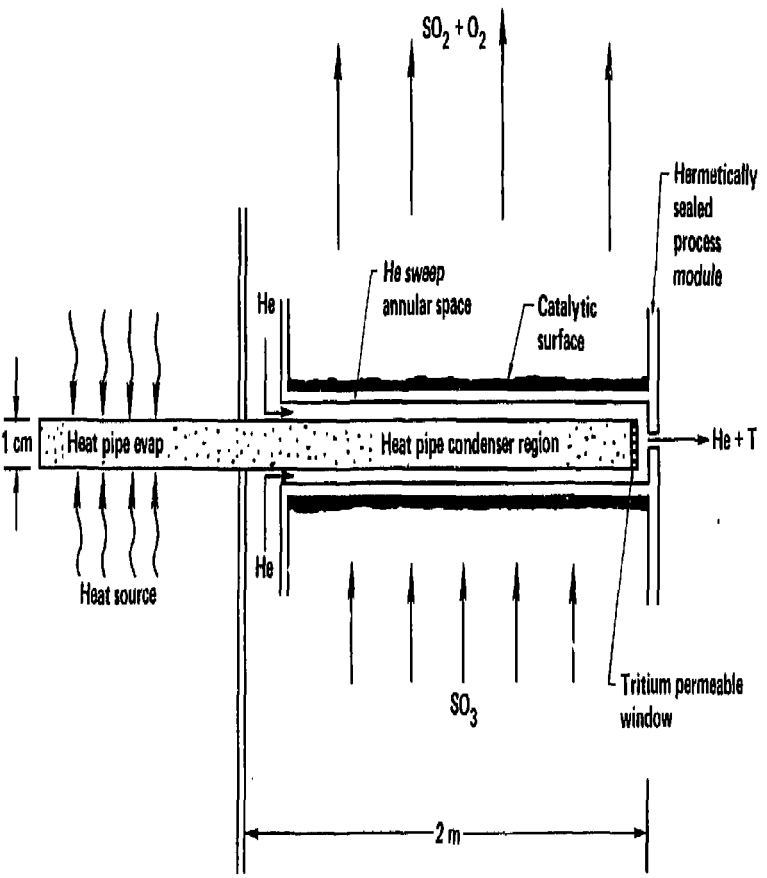

Fig. 19. Cross-flow catalytic cartridge concept.

The other option is a combined unit. The ΔTs would be the same as above, except they would be additive to give $\Delta T = 143°C$ since we must supply simultaneously the sensible heat and the endothermic heat of reaction. This would force the heat pipe temperature up to 1193K, some 70°C hotter than the option above; however, the cost would be reduced from $46 million to $26 million. Note that both options are simpler and cheaper than the fluidized bed SO_3 decomposer presented earlier at $50 million.

CONCLUSIONS

1. A fluidized bed SO_3 decomposer offers attractive performance and cost.

2. The heat pipe/catalytic cartridge offers a more compact design at lower costs.

3. Hot helium feeding the decomposer is the most desirable from the safety standpoint of isolation and for this design costs around 11¢/GJ are projected for the decomposer.

4. Helium transport piping using a cooled wall (200 K below the transport gas temperature) can be used at a cost of around 12¢/GJ.

5. More optimization work needs to be done in seeking the combined cost minimum with the blanket, transport piping and decomposer all linked together.

ACKNOWLEDGMENTS

We want to take this opportunity to thank Ken McCorkle, John Norman, Ken Schultz and Gottfried Besenbruch at General Atomic for their full cooperation and help; and Oscar Krikorian at LLNL.

This work was performed under the auspices of the U.S. Department of Energy by Lawrence Livermore National Laboratory under Contract W-7405-Eng-48.

REFERENCES

1. "Oil in the Eighties: Tight Supply, Soaring Capital Outlays," Oil & Gas Journal, Nov. 13, 1979, pp. 163-169.

2. D. M. Considine, Ed., "Energy Technology Handbook," McGraw-Hill, 1977.

3. Wolf Hafele, "A Global and Long-Range Picture of Energy Developments," Science 209, July 4, 1980, pp. 767-772.

4. H. Kahn, W. Brown, L. Martel, "The Next 200 Years: A Scenario for America and the World," Wm. Morrow & Co., NY, 1976.

5 E. T. Hayes, "Energy Resources Available to the United States, 1985 to 2000," Science 203, Jan. 19, 1979, pp. 233-239.

6 S. Sussman, B. Rubin, R. L. Cooper and D. M. Nesbitt, "A Study of the Importance of Energy RD and D for the United States," Lawrence Livermore National Laboratory. Tech. Rept. UCRL-52140, Oct. 6, 1976.

7 E. Cook, "The Flow of Energy in an Industrial Society," Sci. Am. 224, No. 3, pp. 135-144, Sept. 1971.

8. T. R. Galloway, "Interfacing the Tandem Mirror Reactor to the Sulfur-Iodine Process for Hydrogen Production," 15th Intersociety Energy Conversion Engineering Conference, August 8-22, 1980, Seattle, Washington.

9. J. F. Pierre and R. L. Ammon, Westinghouse Co., Pittsburgh, PA, private communication, December, 1979.

10. H. Fedders, K. Hammeke, and E. Sovvidis, Institute for Reactor Studies, Julich, Germany, private communication, December, 1979.

11. D. R. O'Keefe, J. H. Norman, and D. G. Williamson, "Catalysis Research in Thermo-Chemical Water-Splitting Processes," Rept. GA-A15722, General Atomic Company, January, 1980.

12. J. H. Norman, K. J. Mysels, R. Sharp, and D. Williamson, "Studies of the Sulfur-Iodine Thermo-Chemical Water-Splitting Cycle," Rept. GA-A15757, General Atomic Company, February, 1980.

13. K. R. Schultz, "Lee Rovner's Back-Reaction Calculations," General Atomic Company, (private communication, FD&T/80-37, May 8, 1980).

14. D. Van Velzen, H. Langenkamp, G. Schutz, D. Lalonde, J. Flamm, and P. Fiebelmann, "Development and Design of a Continuous Laboratory-Scale Plant for Hydrogen Production by the Mark-13 Cycle," Int-J-Hydrogen Energy 5, pp. 131-139 (1980).

15. J. H. Norman, K. J. Mysels, D. R. O'Keefe, S. A. Stowell, and D. G. Williamson, "Chemical Studies on the General Atomic Sulfur-Iodine Thermo Chemical Water-Splitting Cycle," Proceedings of the Second World Hydrogen Energy Conference, Vol. 2, August 21-24, 1978, Zurich, Switzerland, pp. 513-543.

16. A. S. Foust, L.A. Wenzel, C. W. Clump, L. Maus, and L. B. Anderson, "Principles of Unit Operations," Wiley, 1960.

17. G. H. Besenbruch, General Atomic Company, (private communication, December 12, 1979).

18. K. H. McCorkle, General Atomic Company, (private communication, January 10, 1980).

19. W. M. Rogers, "Catalysts for Thermo-Chemical Energy," Englehard Industries West, Inc., Hayward, California (private communication, June 5, 1980).

20. A. E. Sherwood, B. G. Monahan, R. A. McWilliams, F. S. Uribe, and C. M. Griffith, "Catalytic Oxidation of Tritium in Air at Ambient Temperature," Lawrence Livermore National Laboratory, Rept. UCRL-52811, July, 1979.

21. O. Levenspiel, "Chemical Reaction Engineering", Wiley, New York, Second Edition, 1972.

22. D. Kunii and O. Levenspiel, "Fluidization Engineering," Wiley, New York, 1969.

23. T. R. Galloway and B. H. Sage, "A Model of the Mechanism of Transport in Packed, Extended, and Fluidized Beds," Chem. Eng. Sci., 25, pp. 495-516 (1970).

24. E.R.G. Eckert and R. M. Drake, "Heat and Mass Transfer," McGraw-Hill, New York, 1959.

25. R. W. Werner, Editor, "Scoping Design of a Tandem Mirror Reactor - Driven Thermochemical Plant for Hydrogen Production," LLNL Tech Rept. in preparation, October, 1980.

26. N. B. Vargaftik, "Tables on the Thermophysical Properties of Liquids and Gases," John Wiley and Son, Inc., 1975.

27. E. R. G. Eckert and R. M. Drake, "Analysis of Heat and Mass Transfer," McGraw-Hill Book Co., 1972.